Journal of Archaeological Science 120 (2020) 105192

Contents lists available at ScienceDirect

Journal of Archaeological Science

journal homepage: http://www.elsevier.com/locate/jas

# The provenance of early Iron Age ferrous remains from southeastern Arabia

Ivan S. Stepanov [a,*], Lloyd Weeks [a], Kristina A. Franke [a], Bruno Overlaet [b], Olivier Alard [c,d], Charlotte M. Cable [a], Yaaqoub Yousif Al Aali [e], Mansour Boraik [e], Hassan Zein [e], Peter Grave [a]

[a] *Archaeomaterials Science Hub, Archaeology & Palaeoanthropology, School of Humanities, Arts & Social Sciences, University of New England, Armidale, New South Wales, 2351, Australia*
[b] *Royal Museums of Art and History, Belgium*
[c] *Department of Earth and Planetary Sciences, Macquarie University, Sydney, New South, Wales 2109, Australia*
[d] *Geosciences Montpellier, CNRS & Université de Montpellier, 34095, France*
[e] *Dubai Municipality, Dubai, United Arab Emirates*

ARTICLE INFO

*Keywords:*
Corroded iron
Iron provenance
Slag inclusions
Southeastern Arabia
Luristan
Iron Age
LA-ICP-MS

ABSTRACT

Recent excavations at Saruq al-Hadid, Dubai, have recovered more than 200 kg of ferrous remains from early Iron Age contexts dated to c. 1250-800 BCE, transforming our understanding of the scale of early iron use in southeastern Arabia. Many of these ferrous artefacts show typological parallels with contemporary objects from Luristan in western Iran, and the possibility of their long-distance import from this well-known iron producing and using region has long been recognized. The present study uses material from Saruq al-Hadid and the contemporary site of Muweilah to explore the provenance of the earliest iron from southeastern Arabia, by (i) summarizing the evidence for the iron resources and technology in the region and adjacent areas; and (ii) compositionally analysing iron ores, iron slags and slag inclusions in artefacts from Saruq al-Hadid and Muweilah, alongside Iron Age ferrous artefacts from Iran, using OM, SEM-EDS, XRF, ICP-MS and LA-ICP-MS. Multivariate statistical analyses are used to explore these geochemical data, alongside a large dataset of ores and artefacts derived from existing geochemical and archaeological publications. The study identifies slag samples from Muweilah as originating from iron smithing activities, providing the first evidence for iron working of any kind in southeastern Arabia. Differences in the geochemical compositions of the material from Saruq al-Hadid and Muweilah and iron ores from the U.A.E. and Oman – particularly the distribution of rare earth elements – suggest that Iron Age ferrous artefacts from southeastern Arabia were not smelted from locally-available iron ores. Rather, the study demonstrates geochemical similarities between southeastern Arabian iron objects, contemporary objects from Luristan, and ores of the Sanandaj-Sirjan metallogenic belt of Iran, suggesting that iron may have been imported, at least partially as complete objects, from this region. Multiple source deposits are indicated, however, and the possible contribution of iron from other regions of ancient Western Asia and neighbouring regions remains to be further explored. The research provides critical new information regarding the long-distance exchange contacts of southeastern Arabia society during the floruit of the early Iron Age, in the late second and early first millennia BCE.

## 1. Introduction

In southeastern Arabia, the origins and earliest adoption of iron technology remain obscure. Several decades ago, an apparent dearth of ferrous remains at local Iron Age (c. 1250-300 BCE) sites prompted Lombard (1989) to describe this period in southeastern Arabia as "L'âge du fer sans fer" (an Iron Age without iron). Despite considerable archaeological excavation in the region in the 30 years since Lombard's pioneering synthesis, with a few notable exceptions ferrous finds from local archaeological sites remain very rare. This local scarcity has been used to suggest that early iron artefacts recovered were obtained through exchange with neighbouring iron-producing regions such as Iran, and that indigenous iron smelting was not practiced in southeastern Arabia until the subsequent Hellenistic Period, when ferrous remains and production residues become more common (e.g. Lombard, 1989; Magee, 1998; Yule and Weisgerber, 2015: 26).

* Corresponding author.
*E-mail address:* ivanstep208@yandex.ru (I.S. Stepanov).

https://doi.org/10.1016/j.jas.2020.105192
Received 8 December 2019; Received in revised form 22 April 2020; Accepted 16 June 2020
Available online 3 July 2020
0305-4403/

Factors considered to have contributed to the relatively late adoption of iron in southeastern Arabia include lack of local knowledge and iron smelting experience, local scarcity of appropriate iron ores, and the high 'investment' costs of ferrous metallurgy in comparison to the strong local tradition of copper smelting and alloying that allowed self-sufficiency in metal production (Lombard, 1989). In contrast to the eastern Mediterranean and the Levant, the economic and political situation in southeastern Arabia also lacked additional contingent factors – including disruptions to palace-oriented metal exchange networks and the collapse of centres of iron technology, such as the Hittite Empire – that provided a complex background to the diffusion of iron technology after 1200 BCE in other areas of ancient West Asia (e.g. Van De Mieroop, 2007: 202–203, Waldbaum, 1999; Erb-Satullo, 2019).

However, the picture of early iron use in southeastern Arabia has been dramatically altered by the recent archaeological excavations of the site of Saruq al-Hadid in southern Dubai (Fig. 1), which has produced more than 200 kg of ferrous remains in the form of fragments and complete weapons from Iron Age contexts dated to c. 1250-800 BCE (Al-Khraysheh and An-Nashef, 2007; Nashef, 2010; Weeks et al., 2019b, 2017). This unprecedented assemblage casts a new light on the scale and access to iron technology in early Iron Age southeastern Arabia, and its analysis offers a unique opportunity to scientifically explore the nature and origins of the earliest iron used in the region.

Here, analyses of the ferrous assemblages from Saruq al-Hadid, and the contemporary Iron Age site of Muweilah (where small-scale iron residues have been discovered), provide a springboard to evaluate the provenance of ferrous remains from Iron Age southeastern Arabia. The study: (i) summarizes the archaeological evidence for the use of iron within the region and in neighbouring areas; (ii) presents new archaeometric analyses of artefacts, production residues, and ore samples from Saruq al-Hadid, Muweilah and other sites in the U.A.E., Oman and Iran; (iii) incorporates previously published geochemical studies to assess individual local and non-local iron ore deposits and occurrences as potential sources; and (iv) discusses the implications of this integrated research.

## 2. The evidence for iron in Iron Age southeastern Arabia

Lombard (1989) and Magee (1998) have summarised the limited evidence from 20th Century excavations for iron artefacts from Iron Age contexts in southeastern Arabia. In the two decades since their work, small-scale ferrous remains have been newly recovered or published from several sites across the region (Table 1), generally reinforcing previous observations about the comparatively small scale and limited nature of iron use in Iron Age southeastern Arabia. They have also re-emphasized links to western Iran and the association between iron, "luxury items" and a snake cult widespread in southeastern Arabia in the Iron Age (Benoist, 2007).

However, ferrous assemblages from two other sites – Muweilah and

**Table 1**
Ferrous remains from Iron Age contexts in southeastern Arabia excavated or published since 1998.

| Site | Iron finds | Reference |
|---|---|---|
| Al Qusais (U.A.E.) | Five arrowheads and one awl from the "Mound of the Serpents". | Taha (2009): 127; Nashef (2010) |
| Jebel al-Buhais (U.A.E.) | One knife/dagger (tomb BHS27), one dagger (BHS46), one dagger (BHS51), one long pin (BHS78), one large socketed spearhead and fragments of another (BHS85). | Jasim, 2012: 91, 139, 298, figs. 310 and 318 |
| Husn Salut (Oman) | Two knife blades and one possible hilt. | Sasso (2018): 312; Condoluci (2018): 222 |
| Jabal Mudhmar (Oman) | One bronze-iron bimetallic dagger with mushroom-shaped hilt. | Gernez et al. (2017) |
| 'Uqdat al-Bakrah (Oman) | A total of 18 fragments, including: one bimetallic Luristan-type dagger (#241), one flanged hilt (#459), one bimetallic blade/hilt (#454), and two blades (#474, 475). | Yule (2018): 34, 142. |
| Tawi Raki (Oman) | Three unspecified artefacts. | Unpublished, noted by Yule (2018): 142 |

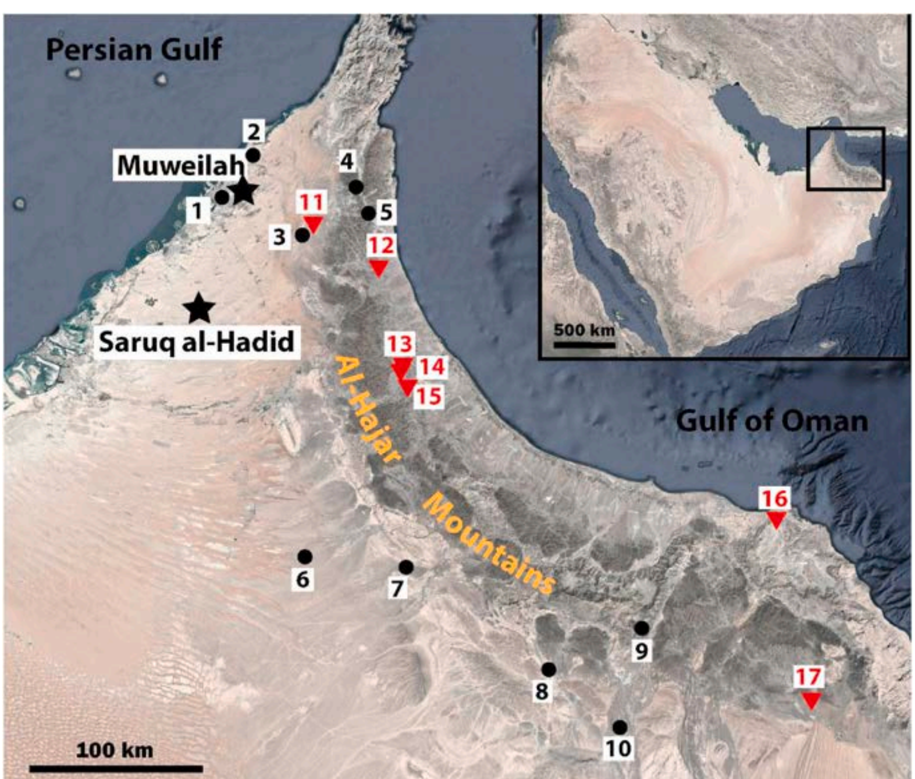


**Fig. 1.** Map of archaeological sites and geological iron ore deposits and occurrences mentioned in the text. The archaeological sites of Saruq al-Hadid and Muweilah (black stars) are those from which samples have been analysed. Other archaeological sites mentioned in the text (black circles): 1. Al-Qusais, 2. Tell Abraq, 3. Jebel Buhais, 4. Masafi, 5. Bithnah, 6. 'Uqdat al-Bakrah, 7. 'Ibrī/Selme, 8. Salut, 9. Tawi Raki, 10. Jabal Mudhmar. Geological sites (red triangles): 11. Ironstones. U.A.E. Jebel Faya, 12. Gossans, U.A.E. Hilu, 13–15. Gossans, Oman: Bayda (13), Arja (14), Lasail (15), 16–17 Laterites, Oman: Ibra (16), al-Russayl (17). (For interpretation of the references to colour in this figure legend, the reader is referred to the Web version of this article.)

Saruq al-Hadid – are different in nature and/or scale from those found elsewhere in the region. As discussed below, this evidence broadens our understanding of the adoption and local development of iron technology in the region.

Excavations at Muweilah, located in the Sharjah Emirate, 15 km from the modern coastline, revealed a complex, relatively short-lived fortified Iron Age settlement. Established by the 10th century BCE, the site was destroyed by fire most probably in the 8th century BCE (Karacic et al., 2018a). The ferrous assemblage from Muweilah consists of around 20 small iron artefacts, including knives, small blades, and pins. This assemblage is similar in nature and context to the other small-scale ferrous remains presented in Table 1: it was found in the columned hall (Building II) in which other luxury and ritual goods, including clay vessels with snake appliqué decoration, bridge-spouted ceramic vessels, and incense burners were also found (Magee et al., 2002: Fig. 30). This building is suggested to have been used by local elites for collective gatherings, feasting ceremonies and administration through the distribution of luxury goods (Magee, 2003; Karacic et al., 2018a: 41).

Of greater significance is the recent identification in the Muweilah assemblage of a small amount (less than 50 g by weight) of possible iron slag, along with a boulder covered with rusty stains that may have functioned as a hammer or an anvil for ferrous metalworking (Fig. 2). All such material comes from a small area of the site ca. 6 m west of the south gate (near rooms 52 and 53, Karacic et al., 2018a: Fig. 2), which was probably the location of a small iron smithy within the settlement.

The preliminary identification of the Muweilah slags as originating from iron-smithing is based upon several macroscopic indicators. Firstly, the slags have an uneven, 'bulgy' surface lacking the visible traces of flow that characterise the majority of tap slags from primary iron smelting (Bayley et al., 2001: Fig. 14). Rather, the earthy and rusty texture of the slags, along with the total absence of vitrification, indicates a high iron content and the likelihood that they were pieces of iron detached and oxidized during smithing (Serneels and Perret, 2003). Secondly, the slags are characterized by an amorphous morphology characteristic of residues found at smithing sites, where it may comprise up to half of the slag recorded (Dunster and Dungworth, 2012: 3). Lastly, the overall small quantity of slag recovered, along with the absence of smelting furnace linings or other technical ceramics, suggests that these residues were produced in a small installation, more typical of smithing hearth than of a smelting furnace. Despite the small scale of these remains, they represent the first firm evidence for local iron working in Iron Age southeastern Arabia.

Saruq al-Hadid, located in the dune fields on the southern border of Dubai (Fig. 1), flourished as a centre for (multi-)community gatherings and ritual activities during the late second and early first millennia BCE (Weeks et al., 2019a, 2019b). The site is best known for the abundant material assemblage associated with these activities, including thousands of artefacts in copper alloy, gold, ceramic, shell, bone, wood, as well as an exceptional abundance – c. 200 kg comprising more than 10, 000 fragments – of ferrous remains (Weeks et al., 2017). The site's ritual paraphernalia associated with a snake cult parallels but significantly exceeds in scale similar finds from other Iron Age sites in southeastern Arabia including Masafi, Bithnah, 'Uqdat al-Bakrah, Jebel Mudhmar and Husn Salut (Benoist, 2007; Benoist et al., 2015; Gernez et al., 2017; Sasso, 2018; Yule, 2018).

The ferrous remains from Saruq al-Hadid are found in different stratigraphic position and in two forms: 1) in Horizon I as broken fragments occurring with copper smelting slags and other artefactual remains; and 2) in Horizon II (c. 1000-800 BCE) and more rarely in Horizon III (c. 1250-1000 BCE) as complete objects occurring with artefacts in other materials, including numerous ceramic vessels and copper-base objects incorporating snake imagery (Weeks et al., 2019a, 2019b; Stepanov et al., 2019a). Recent macroscopic and archaeometric analyses of material from all excavations at the site to date (Stepanov et al., 2019a; Weeks et al., 2019a) suggest that the ferrous remains from Horizon I are residues from late or post-Iron Age scavenging and re-processing to assess the metal content of complete objects, including long iron swords, that were originally ritually deposited earlier in the Iron Age (Horizons II and III).

Previous researchers have interpreted Saruq al-Hadid as a centre for iron-working during its Iron Age and/or post-Iron Age occupation (Nashef, 2010; Herrmann et al., 2012). However, despite the large volume of ferrous remains excavated and studied from the site – and allowing for the possibility that future excavations there may uncover new evidence – several key considerations suggest that iron artefacts were *not* fabricated at Saruq al-Hadid. The absence (to-date) of any ironworking residues, including smelting or smithing slags, smelting installations, smithing hearths or furnace walls (Weeks et al., 2017: 51) is the major argument against iron working on site at Saruq al-Hadid. Secondary evidence relates to the nature of the site's iron artefacts, particularly the recovery of at least two dozen iron swords, up to 1.2 m long, whose manufacture would have required advanced forge-welding skills, for which no evidence is attested in southeastern Arabia at this time other than the small-scale remains from Muweilah. These artefacts, along with other ferrous, bimetallic and bronze weaponry from Saruq al-Hadid such as swords and daggers with mushroom-shaped pommels or handles decorated with ram heads/feline figurines, display distinct stylistic parallels with ferrous and bimetallic objects from Iron Age

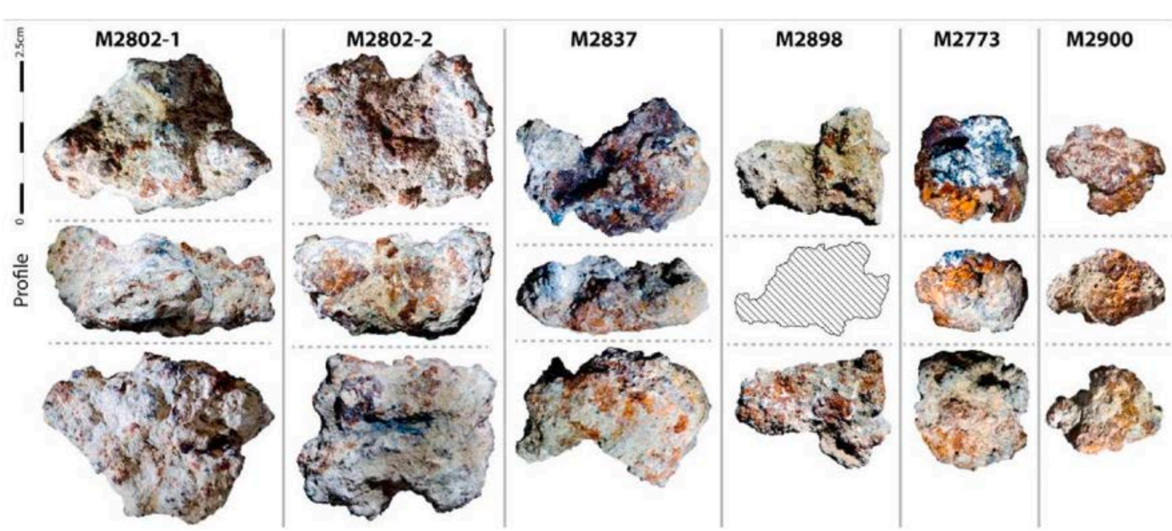


**Fig. 2.** The assemblage of iron slags from Muweilah.

Luristan (1000-800 BCE; Weeks et al., 2017: Fig. 21, Overlaet, 2003: 156, Fig. 123, Muscarella, 1988: Fig. 219), a region known for its advanced early metalworking traditions (see *section* 3). The parallels with Iranian material are not only stylistic, but also technological: comparable fabrication techniques are observed for the Saruq al-Hadid ferrous objects and Iron Age decorative swords from Luristan (Stepanov et al., 2019b). This is reflected in the presence of spheroidized cementite particles and larger ferrite grains indicating annealing at subcritical temperatures (i.e., below 727 °C), and the use of rivets and perishable organic inlays to manufacture blade hilts. These observations were based on the archaeometric study of more than 20 ferrous artefacts and the visual examination of several dozen additional objects and comparisons with previously published studies of Luristan material (e.g., Smith, 1971).

Overall, the collected archaeological evidence from southeastern Arabia – including the small-scale material published in the last two decades and the assemblages from Muweilah and Saruq al-Hadid – enhances but does not overturn existing conceptions of the earliest iron use in the region. It remains unlikely that indigenous iron smelting (primary production) was undertaken in southeastern Arabia during the Iron Age, although Muweilah provides evidence for nascent, small-scale local iron working (i.e., secondary production) at this time. The available evidence thus reinforces the possibility that these earliest iron objects were imports, while the material from Saruq al-Hadid highlights the need to identify more precisely the source region and to revise dramatically upwards our conception of the scale of such exchanges.

A final note regarding the possibility of local iron production in southeastern Arabia is warranted. While Lombard (1989) was broadly correct to observe that good iron ores are rare in southeastern Arabia, it should be noted that several ironstone and lateritic iron occurrences are recorded in the U.A.E. and Oman (Fig.1) (Ploquin et al., 1999; Al-Khirbash, 2015, Al-Khirbash, and Semhi, 2018). Thin (up to 1 m) beds of ironstones, associated with limestones, occur in the Jebel Faya range (~40 km from Muweilah and ~100 km from Saruq al-Hadid), while moderately thick (up to 70–100 m) iron oxide rich laterite beds developed after peridotites or gabbros are known in various locations within the Semail Ophiolite in Oman. However, it should be stressed that no archaeological evidence for the exploitation of these deposits has been identified. Within the ophiolite, iron-rich gossans also cap the massive sulphide deposits (Lippard et al., 1986: 127, Robins et al., 2006: 21–36, Wilson, 1997: Table B1). The latter were intensively exploited for copper during the Iron Age, based on the evidence of smelting sites and the high iron content of local raw copper (Benoist et al., 2015; Weisgerber, 2008, Weeks, 2003). Thus, primary iron production in southeastern Arabia using local ores was possible, and such sources must be included in any programme exploring the provenance of archaeological iron from the region.

## 3. Early iron technology in neighbouring regions

Consideration of the state of Iron Age iron technology in Iran and other regions adjacent to southeastern Arabia provides a critical foundation for the discussion of the origin of the earliest iron at Saruq al-Hadid and contemporary sites in the U.A.E. and Oman. The recent comprehensive synthesis by Erb-Satullo (2019) obviates the need for an in-depth review of patterns of iron adoption in the northern regions of West Asia. By the late second to early first millennium BCE, smelted iron was utilized, with uneven frequency, over a wide area stretching from the eastern Mediterranean to Anatolia, Iran and beyond (Erb-Satullo, 2019: Fig. 6, see also Waldbaum, 1999, Moorey, 1994: 278–292). However, occurrences of early iron artefacts from several regions adjacent to southeastern Arabia – including southern Iran, southern Mesopotamia, the Arabian Peninsula and adjacent islands, and India – are not considered in Erb-Satullo's review. This evidence is thus presented in some detail below, along with a consideration of the distribution of related iron ore deposits with evidence of pre-modern exploitation.

As noted by Erb-Satullo, 2019 (see also Overlaet, 2004), the adoption and expansion of iron use in northwestern Iran, Kurdistan and Luristan is securely attested by 10th-9th centuries BCE. These early developments likely reflect the abundance of iron ore sources in Iran (Fig. 3, Nabatian et al., 2015; Ghorbani, 2013: 249, Pigott, 2004). Iron resources of the northern and west-central Zagros, particularly those occurring east of the Zagros thrust belt within the so-called Sanandaj-Sirjan (SRJ) metallogenic belt, include ancient mines first mentioned in records from the 13th Century CE (Allan, 1979: 67, Momenzadeh, 2004).

In contrast to the western and northern Zagros, southwestern Iran, home to the Elamite civilization, lacks large iron ore deposits (Fig. 3). Iron artefacts are absent from late second and early first millennium BCE archaeological deposits in both lowland and highland southwestern Iran, at Susa (e.g. Miroschedji, 1981), in Mamasani (Weeks et al., 2009; Petrie et al., 2009), and at Tal-e Malyan (Carter and Deaver, 1996). Instead, the widespread adoption of iron in this area appears to have taken place after the late eighth century BCE, based on small-scale iron finds at Susa and textual references to iron in Elamite sources c. 650 BCE (Potts, 2004: 260, 277, Miroschedji, 1981: Fig. 40.14 and 15; Pl. XIII.12, 13).

Southeastern Iran, on the other hand, contains several major iron ore deposits (Nabatian et al., 2015), some of which were probably mined as early as Achaemenid and Sasanian times (Ghorbani, 2013: 68–69). However, settlement in the region remains very sparsely documented during the key period of interest from c. 1300-800 BCE (Magee, 2013: 494, Maresca, 2018), with the consequence that iron artefacts are not recorded in the region at this time.

Evidence for early iron use in southern Mesopotamia (Babylonia) is equally sparse. The situation parallels that in lowland southwestern Iran, with significant iron use emerging clearly only in the Neo-Babylonian period (626-539 BCE), when written sources indicate the replacement of bronze by iron for use in weaponry and some household implements (Curtis, 2013: 142–143, Moorey, 1994: 290). This may, in part, reflect the distribution of iron sources within greater Mesopotamia, which are mainly known from northern regions (Al-Bassam and Hak, 2006; Maxwell-Hyslop and Mallowan, 1974; Skoček et al., 1971). Under Assyrian rule in the late second and early first millennia BCE, these areas probably contributed to the large scale iron use attested by Neo-Assyrian historical sources and archaeological evidence (Erb-Satullo, 2019).

In the Arabian Peninsula and adjacent islands, with meagre evidence for the early use of iron, iron ores are known from several areas in Arabian Shield rocks of western Saudi Arabia (Moufti, 2010; Edgell, 2006: 16–17, duBray et al., 1991). Possible ancient iron mines and production sites have been reported from the central, western and southwestern provinces (Zarins et al., 1980: 27, Hester et al., 1984: 115, Table 1), although most date to the Abbasid period based on surface material. Smelting of local ores was also ethnographically documented in the southwestern part of the region (e.g. Dostal, 2002). In northwestern Yemen, piles of iron slag of unspecified age were discovered near the As-Sarat lateritic field (Overstreet et al., 1976). While rare, iron objects are also found as early as the time of the south Arabian Kingdoms in the first millennium BCE (Antonini de Maigret and Robin, 2015). The pattern of iron use on Bahrain Island is similar to that of southeastern Arabia: although very rare iron artefacts are known from as early as the mid-second millennium BC (Qala'at al-Bahrain Period III) and early first millennium BCE (Period IV), iron becomes common only in the post-Iron Age or Hellenistic period (Period V, Højlund et al., 1994: 382, Figs. 1881–1885, Højlund and Andersen, 1997: 147, Figs. 692 and 697). A ferrous sword, typologically similar to examples from Saruq al-Hadid and Luristan, was recovered from the Late Dilmun (1000-400 BCE) site of Al-Hajjar 1 (Lombard, P., Kervan, M., 1989: 78, nos. 144–145; Rice, 1988: Pl. XI). Mesopotamian documents from the time of Sennacherib (704–681 BCE) further suggest the scarcity of iron in Bahrain at this time, noting that labourers who travelled to Mesopotamia from Dilmun were equipped with bronze, rather than iron, tools and implements (Potts, 2009a: 36).

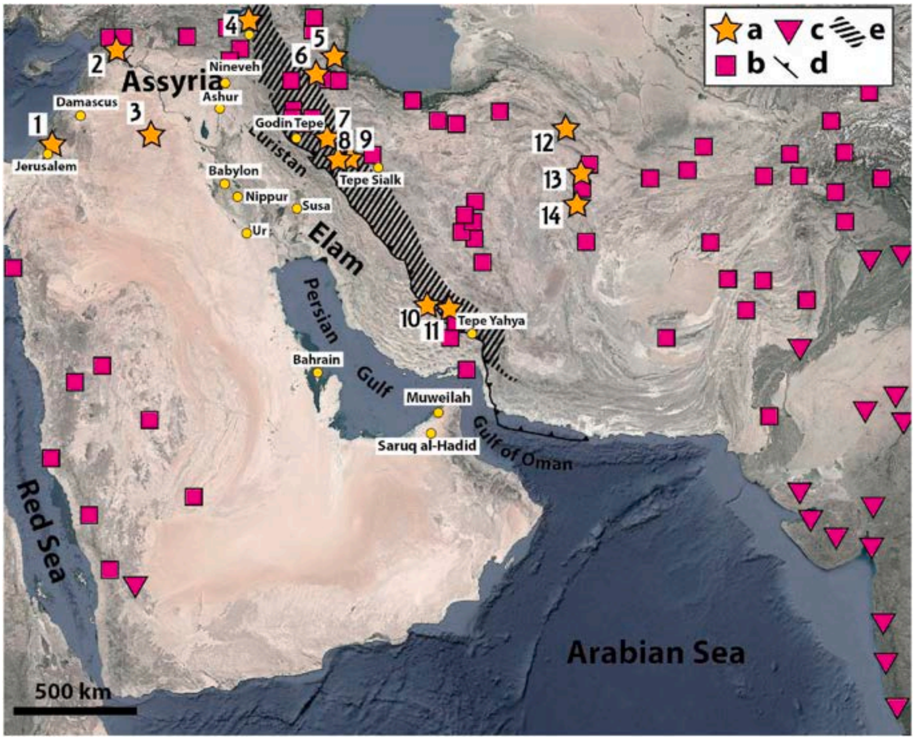


**Fig. 3.** Location of important geological iron resources and iron mines exploited at different periods in the past in regions neighbouring southeastern Arabia. (a) Mines exploited in the past: 1. Jordan, Mugharet el-Wardeh, 2. Syria, Kerry, 3. Iraq, Hussainiyat, 4. Turkey, Van, 5–14. Iran; 5. Masuleh, 6. Kavand, 7. Ahangaran (East Malayer), 8. Shamsabad, 9. Khugan, 10. Neiriz, 11. Golegohar, 12. Pivezhan, 13. Ahangaran (East Iran), 14. Sangan. (b) Large iron ore deposits. (c) Past iron smelting sites. (d) Zagros thrust belt. (e) Sanandaj-Sirjan (SRJ) metallogenic belt. Map compiled from data presented in Nabatian et al, 2015), Momenzadeh (2004): Fig. 7, Maxwell--Hyslop and Mallowan, 1974, Skoček et al. (1971), Al-Amri (2008), Overstreet et al. (1976), Moufti (2010), Abdulhay and Zahrani, 2005, Malkani and Mahmood (2016), Belli (1991). For India, pre-20th century iron smelting sites are shown, rather than modern ore deposits (based on data from Chakrabarti, 1992: Fig. 13).

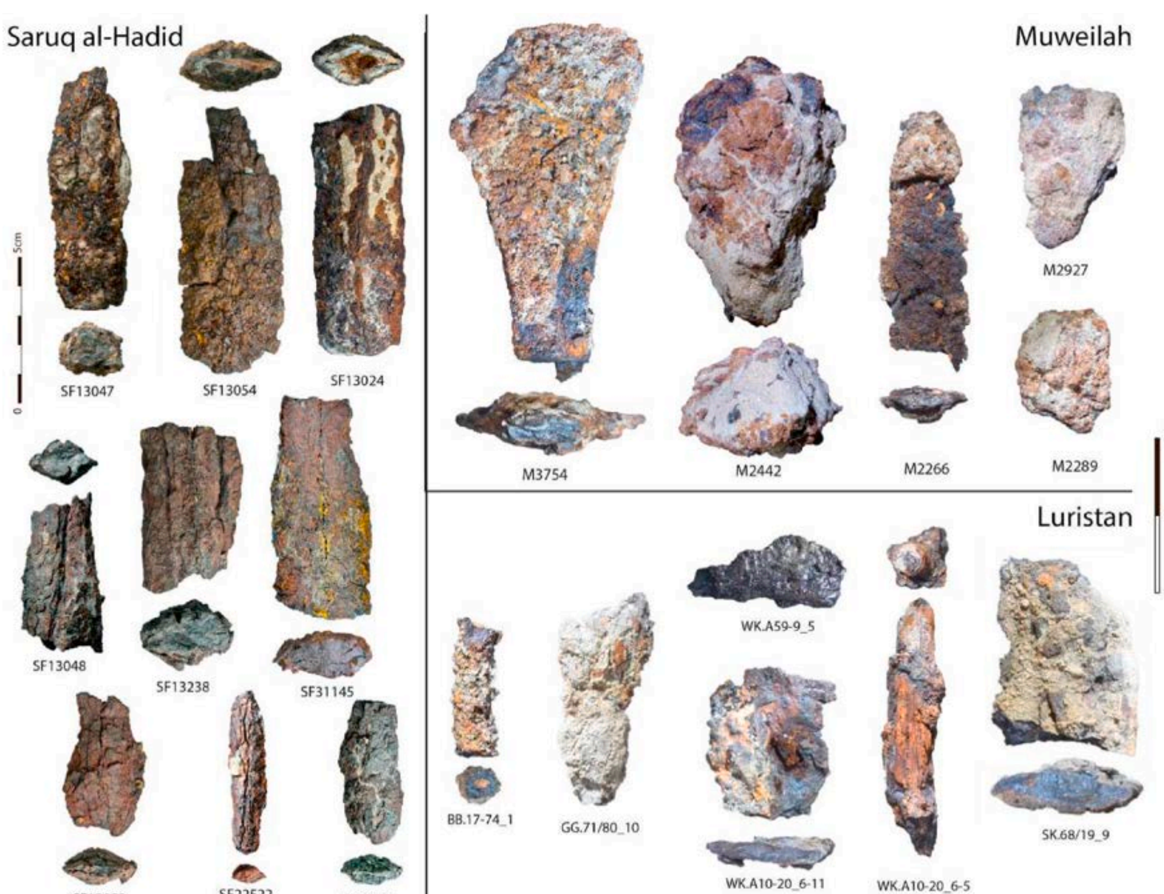


**Fig. 4.** Archaeological materials from Saruq al-Hadid, Muweilah and Luristan investigated during the study. For Saruq al-Hadid, only a sub-set of typical artefacts is shown. For Luristan artefacts: BB = Bard-i Bal; WK = War Kabud; GG = Ghaluli Gulgul; SK = Sar Kabud.

Finally, South Asia is a region rich in iron resources including both large and small deposits (Chakrabarti, 1992: 23–35), in which iron smelting technology was locally developed and used across a vast territory by the last quarter of the second millennium BCE (Tewari, 2003, 2010). The early South Asian advance of iron-making can be also seen through the production of crucible steel, possibly by the second half of the first millennium BCE (Srinivasan and Ranganathan, 2004).

Thus, with the exception of South Asia, few regions adjacent to early Iron Age southeastern Arabia provide evidence for the availability and exploitation of ore resources, significant histories of iron use, or the technological trajectories leading to the early adoption of this new metal. When viewed alongside the geochemical patterns discussed below (*section 5.2*) and within the socio-cultural context of Iron Age southeastern Arabia (*section 2*), this evidence contributes to considerations of the provenance of early iron present in southeastern Arabia.

## 4. Materials and methods

Archaeometric analyses were conducted to: 1) identify the nature of the ferrous residues from Muweilah macroscopically identified as iron smithing slags, 2) to characterise the composition of locally available iron ores, and 3) to determine provenance patterns for iron artefacts from Saruq al-Hadid and Muweilah based on the composition of their slag inclusions (SIs). The compositional data generated were subsequently explored using a variety of statistical analyses, alongside geochemical data incorporated from previously published studies.

Archaeological materials (N = 52, Fig. 4) analysed include broadly contemporaneous Iron Age ferrous artefacts and residues from Saruq al-Hadid and Muweilah in southeastern Arabia, and the sites of Bard-i Bal, War Kabud, Ghaluli Gulgul and Sar Kabud in the Pusht-i Kuh, Luristan. Geological resources (N = 21, Fig. 5) sampled in the present study include five iron ore occurrences from the U.A.E. and Oman: ironstones from Jebel Faya (Fig. 5a and b), Fe-rich gossans at Hilu, Lasail and Bayda (Fig. 5c and d) and laterites from Al-Russayl (Fig. 5e). Full data are provided in *Supplementary #1*.

Optical microscopy (OM) was used to investigate the microstructure of the Muweilah slags, and to locate chemically-unaltered slag inclusions in the archaeological objects (Stepanov et al., 2017) in order to facilitate their subsequent major and trace element analyses by SEM-EDS and LA-ICP-MS. The results of the investigation of the microstructure of a sub-set of the ferrous artefact assemblage from Saruq al-Hadid are presented in detail elsewhere (Stepanov et al., 2019b).

### 4.1. Provenance based on slag inclusions (SIs)

To address the question of provenance for iron, analyses were conducted following a now commonplace approach based on analysis of SIs (Dillmann and l'Héritier, 2007; Charlton et al., 2012, Disser et al., 2017). The SIs were analysed by SEM-EDS to determine Si content, and by laser ablation inductively coupled plasma mass spectrometry (LA-ICP-MS) for contents of other major and trace elements. Smithing slags and iron ores from the U.A.E. and Oman were analysed at the ALS Minerals laboratory (Brisbane, Australia) via conventional "whole-rock analysis" X-ray fluorescence (XRF) lithium metaborate fusion for major elements followed by ICP-MS for trace elements. The instrumental protocols for the use of SEM and LA-ICP-MS are provided in *Supplementary #2*.

The composition of slag inclusions (SIs) from the artefacts and smithing slags from southeastern Arabia was compared with the composition of iron ores from the U.A.E., Oman, Saudi Arabia, Iran, Iraq,

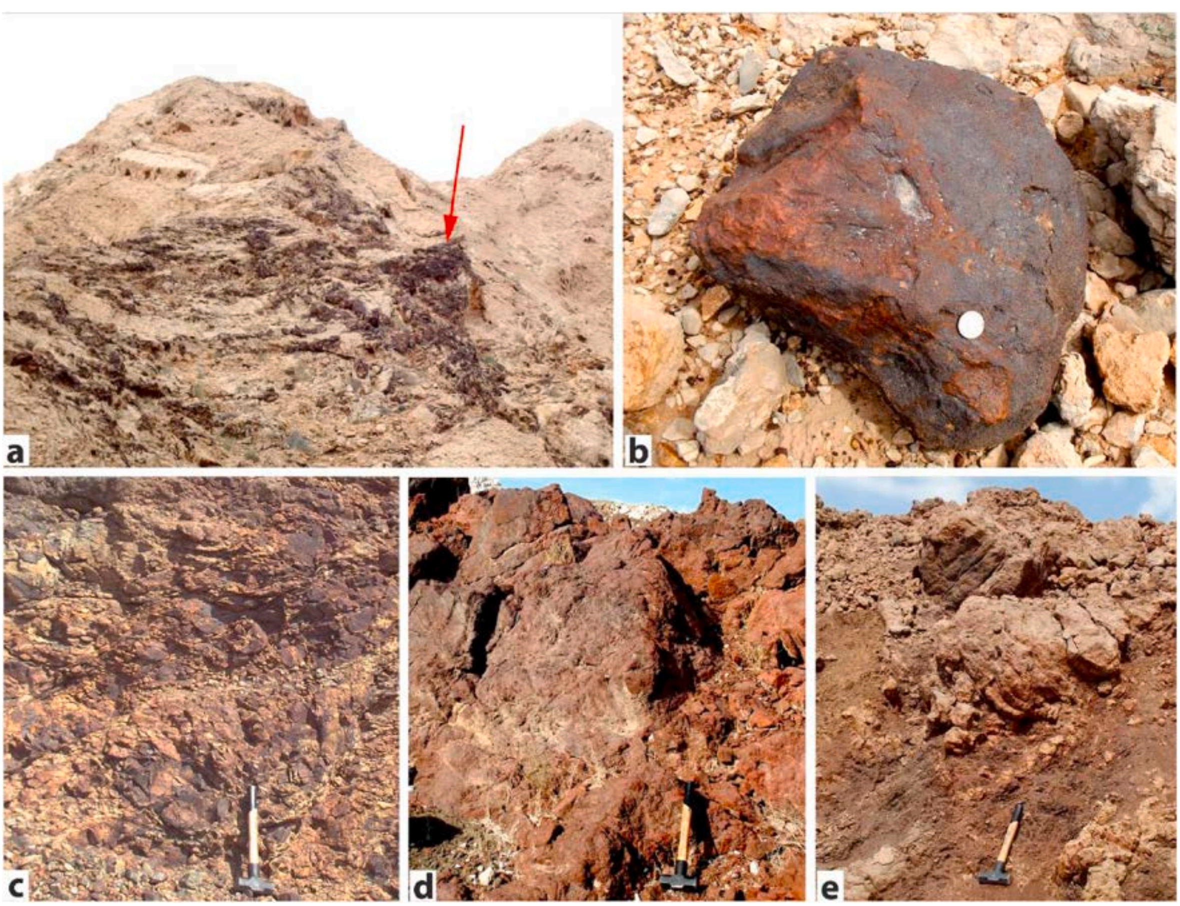

**Fig. 5.** Some iron ore occurrences and deposits visited and sampled for the present study. (a–b). Ironstones, J.Faya (U.A.E.): (a). Bed of ironstones, as shown by the arrow; (b). Eroded ironstone boulder. (c–d). Gossans (Oman): at Lasail (c) and Bayda (d). (e). Laterites (Oman) at Al-Russayl.

Syria, Jordan and India, and with broadly contemporary ferrous objects from Iron Age Luristan in western Iran. The majority of the geochemical data incorporated into our comparisons – especially non-local ores from Western Asia and India, which were not available as physical samples – were taken from previously published geological studies. The full list of newly-generated chemical data and previously published analyses utilized in the present study is provided in *Supplementary #3*.

Comparisons reflect a multi-level approach to provenance assessment, incorporating a regional-level comparison of the Saruq al-Hadid and Muweilah artefacts against possible sources from southeastern Arabia, and a broader-level comparison of archaeological materials against sources from across Western and Southern Asia. Moreover, as some published datasets did not include a fully comparable set of elements, comparisons involved several consecutive steps. During the first step, only analyses of major elements of ores and SIs were compared, permitting provenance assessments against the maximum possible number of ore sources (i.e., especially those lacking trace element data).

The patterns deduced from comparisons of slag inclusions with iron ores based only on major elements were taken with caution, as the contents of most of major elements can be 'polluted' by the composition of the furnace lining and charcoal used in the metallurgical system (Serneels, 1993; Crew, 2000; Charlton et al., 2010). However, previous studies have shown that, despite contamination issues, the analysis of major element concentrations and ratios in slag can differentiate the use of certain ore deposits and types (Buchwald and Wivel, 1998; Disser et al., 2017; Desaulty et al., 2009; Leroy et al., 2012). For example, lateritic ores are often characterized by high Al and Ti contents, which can be also reflected in the slag and slag inclusions (Gordon and Van Der Merwe, 1984). Similarly, Skarn-hosted iron ores are often characterized by high Ca and elevated Mg contents (Mollaei et al., 2009; Zamanian et al., 2007; Barati and Gholipoor, 2013). Contamination from charcoal is regarded as particularly likely in relation to concentrations of Ca, Mg, Na and K, with the latter two elements being generally low in iron ore types commonly exploited in the past (Serneels, 1993; Crew, 2000; Charlton et al., 2010). Nevertheless, certain types of iron ores are associated with salts or can be subject to Na–Ca- or K-alteration resulting in elevated contents of these elements in the ore (Atapour and Aftabi, 2017; Barton, 2013: 525–526).

Taking into account these considerations, and the positive results from other studies that have incorporated major elements for determination of iron provenance (Disser et al., 2017; Dillmann et al., 2017), the major elements considered here in the first provenance step include: Mg, Al, Si, Mn, Ti, Ca, K. Al was included for provenance comparisons because the SIs analysed in the present study did not contain hercynite crystals, which have been associated with Al enrichment in previous studies (Dillmann and l'Héritier, 2007). The contents of these elements in the slag inclusions were reliably measured, due to their abundance (mostly exceeding 0.5 wt% as their respective oxides, except for low Mn in some samples), and the sensitivity of LA-ICP-MS (detection limits < 0.1 wt%). Furthermore, SIs were analysed as bulk area (SEM) and bulk volume (LA-ICP-MS) which generated a signal from both olivine crystals (if present) and the surrounding glass matrix. This allowed the avoidance of potential biases deriving from the analysis of only selected phases in the SIs.

Sodium and phosphorus were not considered for comparison due to the their relatively low contents in slag inclusions (avg. $Na_2O \approx 0.5$ wt%, avg. $P_2O_5 < 0.5$ wt% according SEM-EDS), and higher detection limits for these elements using ICP-MS, SEM-EDS. Overall, the main goal of the first comparison step was to provide an initial insight into provenance, by identifying the most probable ore sources exploited in the past and ruling out the most improbable. The positive patterns deduced during the first step were then further explored during subsequent steps, given the availability of trace elemental data for the same deposits.

The second comparative step used only trace elements (Y, La, Ce, Pr, Nd, Sm, Eu, Gd, Dy, Er, Yb, Th, U) which typically pass from ore into slag unaffected by partitioning or contamination from charcoal or furnace lining (Leroy, 2010: 199, Tab. IV.1; Leroy et al., 2012). Spider diagrams (incorporating REEs + Y, Th and U) were used as part of a separate validation of observed multivariate statistical patterns. During the third comparative step, both major and trace elements were utilized, which added rigour, but also required elimination of several ore sources for which a smaller number of elements had been analysed.

The Aitchison's (1986) centred log ratio transformation, commonly applied in studies dedicated to analyses of slag inclusions (Charlton et al., 2012; Charlton, 2015, Disser et al., 2017, Dillmann et al., 2017; Bauvais et al., 2018), was utilized to normalize elements during the first and third provenance steps:

$$\mathrm{Xij} = \log_{10}\left(X\right) - \frac{1}{N}\left(\left(\log_{10}\left(X_{k1}\right) + \log_{10}(X_{k2}) + \ldots \log_{10}\left(X_{kN}\right)\right)\right)$$

Xij is the normalized content of a given element, $X_k$ is the absolute content of each element included in the cluster analysis. In the first step based only on comparison of seven major elements, N = 7. In the third step based on comparison of both major and trace elements (Y, REE), N = 18 (and calculated Xij were different from the first step). The advantage of this approach is that deciphering of vectors depends on examination of their ratios. This negates the dilution biases imposed by variable amounts of FeO, which is a well-known phenomenon in SIs (Buchwald and Wivel, 1998, Dillmann and l'Héritier, 2007, Charlton et al., 2012: 2284). Finally, in the present study PCA was chosen for clustering instead of bivariate plots (sometimes utilized for iron provenance, e.g., Desaulty et al., 2008: Fig. 8), because PCA values are linearly uncorrelated, unlike variables of bivariate plots, which allows a more consistent grouping.

The log ratio approach also proved useful to partly eliminate the bias from comparison of chemical data obtained by several different methods, such as LA-ICP-MS, used for analyses of SIs, and XRF/solution ICP, used in most published studies of iron ores. Nevertheless, given the methodology of the study, all generated data patterns and inferred provenance assignations are treated with caution.

### 4.2. A note on the alteration of slag inclusions (SIs)

All ferrous archaeological artefacts from Southeastern Arabia investigated in the present study are fully corroded, with virtually no surviving metal, and all analysed SIs are therefore situated in corroded iron masses. Like metallic iron, SIs are subject to alteration in the burial environment due to prolonged contact with water (Dussubieux et al., 2009: 158, Anaf, 2010). A variety of microscopic and compositional analyses demonstrate that altered SIs can be recognized by the lamellar structure of their heterogeneous silicate matrix and related changes to composition caused by leaching. These analyses indicate that altered SIs occurred in almost all archaeological artefacts in the present study. However, analyses also demonstrated that largely unaltered SIs occurred in almost every corroded iron sample, and were especially common in thicker and denser artefacts. The rigorous identification of altered SIs allowed for their exclusion from subsequent analysis, and a focus on the analysis of unaltered SIs facilitated the generation of a robust analytical dataset to support provenance conclusions. *See Supplementary Information #2* for full de*scription of chemical alteration of SIs and Supplementary Information #3* for analyses of altered SIs.

## 5. Results

### 5.1. Investigation of iron-working residues from Muweilah

Investigation of the structure and composition of the Muweilah slags revealed several features commonly reported for slags from the iron-smithing process. The slags incorporate minute islands of metallic iron (Fig. 6d) and amorphous iron corrosion phases, possibly maghemite ($\gamma$-$Fe_2O_3$) and goethite (FeO(OH)) (Figs. 6b and 7d), which is consistent

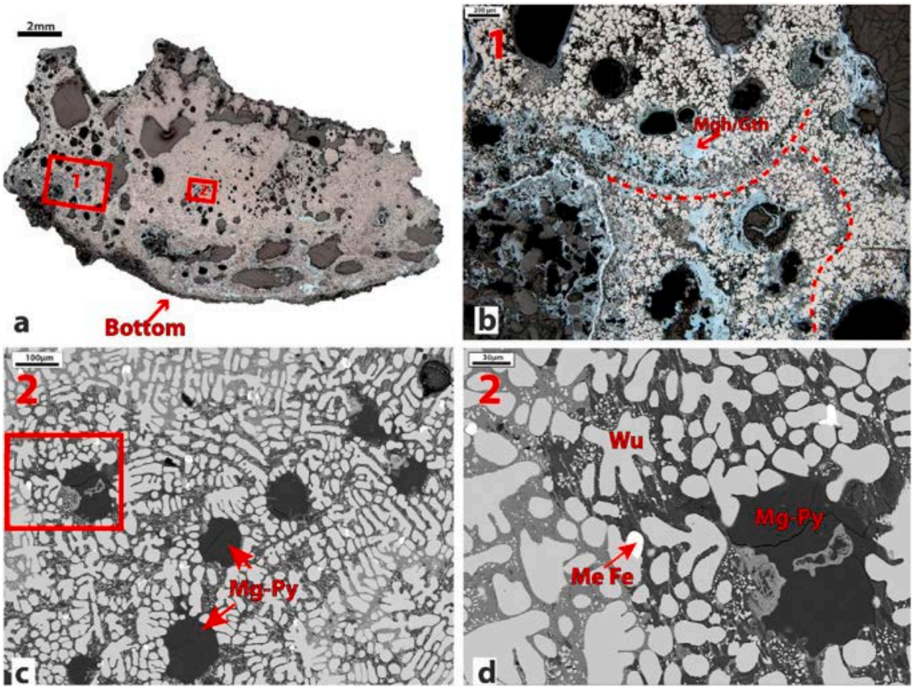


**Fig. 6.** Microstructures of Muweilah slag M2837. (a) OM. Overview image of the cross-section. (b) OM. Magnified area 1 *from (a)* showing incongruently cooled slag layers (separated by a dotted line). (c) SEM-BEI. Magnified area 2 *from* (*a)* showing relics of Mg-pyroxene (Mg-Py) smithing additives in wustite-fayalite matrix. (d) SEM-BEI. Magnified area of red rectangle *from (c)*. Abbreviations: metallic iron (Me Fe), wustite (Wu), maghemite (Mgh), goethite (Gth). (For interpretation of the references to colour in this figure legend, the reader is referred to the Web version of this article.)

with the characteristics of one of three common types of smithing residues. Several Muweilah slags contain hot oxidation layers and lamellar hammerscales (Fig. 7a, e.g. Dungworth and Wilkes, 2007; Bauvais and Fluzin, 2009: Fig. 8.2; Biggs et al., 2013: Fig. 4b). Most slags consist of several, often spheroidal layers of wustite, which cooled incongruently when the slag was viscous, based on the presence of interface layers and sharp differences in the sizes of the wustite globules (Figs. 6b and 7b). These spheroidal layers could represent globular hammerscales detached from the metal during smithing (e.g. Bauvais and Fluzin, 2009: Fig. 8.3; Eekelers et al., 2016: Fig. 3a and b). Overall, these features indicate a highly heterogeneous, oxidizing environment during slag formation, consistent with smithing rather than smelting (McDonnell, 1991; Serneels and Perret, 2003).

Two slags (M2837, M2898) are characterized by distinct base layers incorporating flattened pores and/or fused outer sandy crusts (Fig. 6a, 7c, d). In M2898 a transitional silicate layer, containing newly formed pyroxene and glass, developed at the interface between the slag and the sandy crust (Fig. 7d). Similar crusts occur all over the surface of two other slags (M2802–1, M2900), indicating that these slags are not typical furnace bottoms, but a different type of smithing residue. These fused sandy crusts have silico-calcareous composition consisting of quartz, calcite, plagioclase and clay (Fig. 8a, b, Table 2). Two slags (M2837, M2773) also incorporate inclusions of semi-reacted relict Mg-pyroxene (Fig. 6c, d, Table 2). Since pyroxenes are common in the

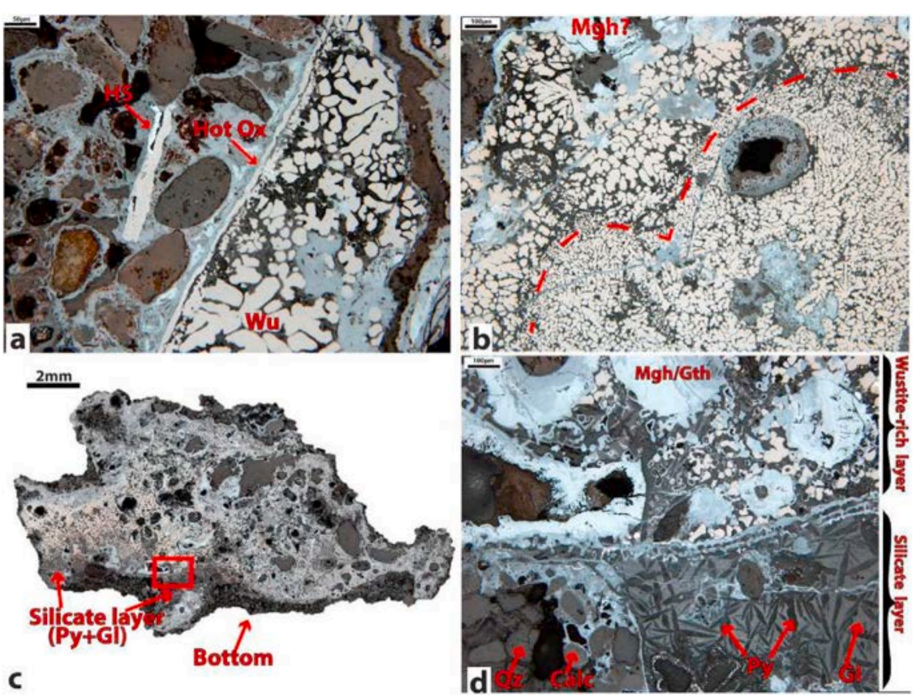


**Fig. 7.** Microstructures of Muweilah slags. (a) OM, M2773. Hammerscale (Hs) and hot oxidation (Hot Ox) layer at the outer surface of slag with designated wustite (Wu). (b) OM, M2773. Dotted line marks the interface of incongruently cooled slag layers; with designated maghemite (Mgh). (c) M898. Overview image of the cross-section. (d) Magnified area of red rectangle *from (c)*. Abbreviations: glass (Gl), pyroxene (Py), calcite (Calc), quartz (Qtz). (For interpretation of the references to colour in this figure legend, the reader is referred to the Web version of this article.)

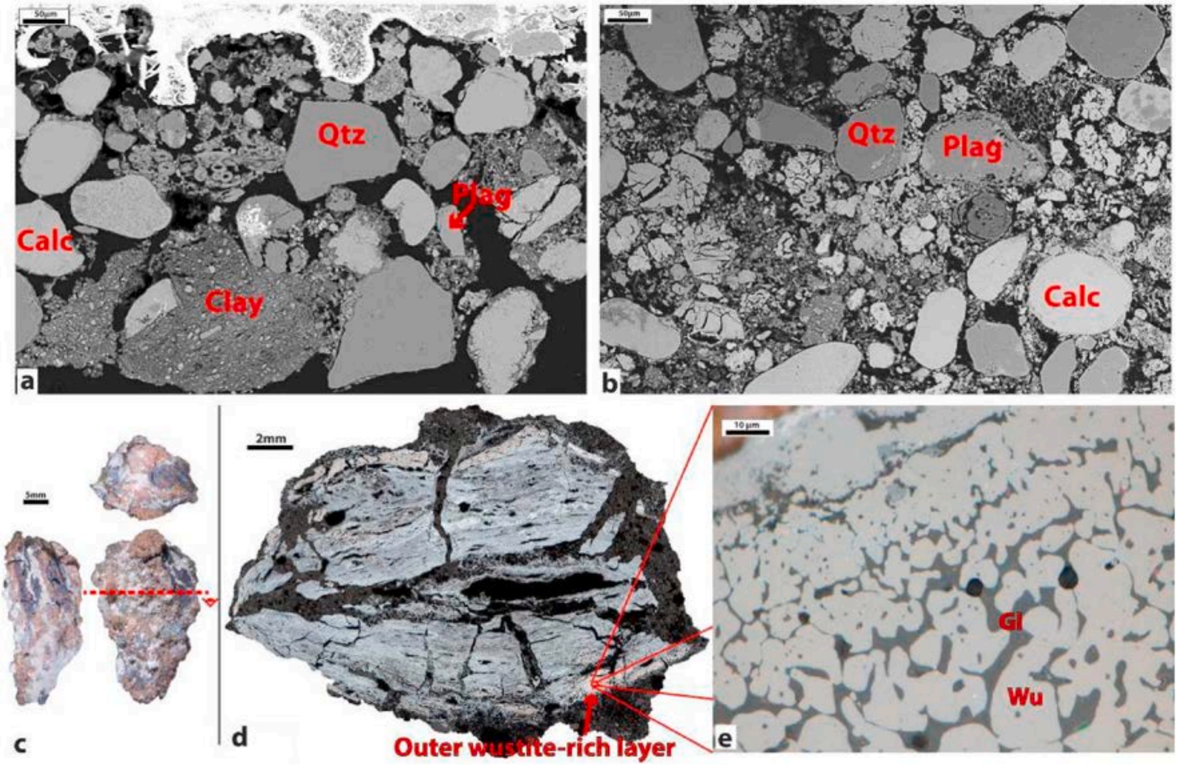


**Fig. 8.** Microstructures and photos of Muweilah residues. a–b: SEM-BEI, microstructures of sandy crusts fused to the outer surface of smithing slags with designated components: quartz (Qtz), plagioclase (Plag), calcite (Calc) and clay. (a) M2898; (b) M2837. c–e: Semi-product M2442: (c) Photo, dotted line marks location of the sample cut; (d) OM, overview image of the cross-section. (e) OM, magnified area of the wustite-rich outer layer, resulting from hot oxidation, shown by arrows *in (d)*, containing wustite (Wu) globules and interstitial Fe-rich glass (Gl).

**Table 2**
Major element composition (wt%) of Muweilah slags and semi-product (M2442) by XRF and SEM-EDS, including key phases and features.

| Sample | Feature | | Analysis | | $Na_2O$ | MgO | $Al_2O_3$ | $SiO_2$ | $P_2O_5$ | CaO | $K_2O$ | $TiO_2$ | MnO | FeO | $SO_3$ | LOI | Tot. |
|---|---|---|---|---|---|---|---|---|---|---|---|---|---|---|---|---|---|
| M2837 | Bulk slag | | XRF | | 0.2 | 2.52 | 1.48 | 7.69 | 0.24 | 0.55 | 5.97 | 0.07 | 0.02 | 69.07 | 1.34 | 1 | 90.17 |
| | Bottom crust | | SEM area an | $\bar{x}$ n = 2 | 0.7 | 3.1 | 2.8 | 35.7 | 2.2 | 47.4 | 0.7 | bdl | bdl | 5.1 | 1.1 | – | 98.8 |
| | Relict Mg-Py | | SEM spot an | | 0.6 | 33.2 | 1.6 | 60.9 | bdl | 0.6 | 0.9 | bdl | bdl | 1.4 | 0.3 | – | 99.5 |
| M2802-1 | Bulk slag | | XRF | | 0.1 | 1.31 | 0.45 | 4.83 | 0.35 | 0.15 | 6.25 | 0.03 | 0.02 | 72.36 | 0.48 | 4.5 | 90.78 |
| | Bottom crust | | SEM area an | $\bar{x}$ n = 1 | 3.2 | 2.8 | 6.4 | 37.4 | 1.7 | 32.8 | 0.4 | bdl | bdl | 11.1 | 2.8 | – | 98.6 |
| M2802-2 | Bulk slag | | XRF | | 0.09 | 1.08 | 0.15 | 2.45 | 0.48 | 0.07 | 4.68 | 0.01 | 0.01 | 80.77 | 0.46 | – | 90.25 |
| M2898 | Bulk slag | | XRF | | 0.14 | 2.61 | 0.55 | 6.93 | 0.6 | 0.25 | 8.37 | 0.03 | 0.04 | 60.4 | 1.34 | – | 81.26 |
| | Transit | new Py | SEM spot an | | 0.4 | 12.4 | 2.7 | 54.4 | 1.6 | 5 | 0.5 | bdl | 0.1 | 21.3 | 0.3 | – | 98.7 |
| | layer | Gl | SEM spot an | | 3.8 | 0.6 | 12.7 | 23.5 | bdl | 17.2 | 4.9 | 0.4 | bdl | 31.2 | 4.8 | – | 99.1 |
| | Bottom crust | | SEM area an | $\bar{x}$ n = 3 | 1 | 4.2 | 3.3 | 41.2 | 2.3 | 40.6 | 0.6 | 0.5 | bdl | 4.3 | 0.8 | – | 98.8 |
| | | | | σ | 0.8 | 1.4 | 1.8 | 13.3 | 0.6 | 11.9 | 0.2 | 0.6 | – | 3.1 | 0.2 | – | |
| M2900 | Bulk slag | | SEM area an | $\bar{x}$n = 11 | 0.1 | 0.7 | 1.2 | 4.7 | 0.6 | 0.2 | 6 | bdl | bdl | 84.8 | 1.1 | – | 99.4 |
| | | | | σ | – | 0.3 | 0.9 | 3.8 | 0.9 | 0.1 | 1.9 | – | 0 | 4.6 | 0.6 | – | |
| | Bottom crust | | SEM area an | | 0.7 | 4.3 | 2.5 | 40.6 | 1.6 | 41.3 | 0.7 | bdl | bdl | 6.1 | 0.8 | – | 98.6 |
| M2773 | Bulk slag | | SEM area an | $\bar{x}$n = 8 | 0.5 | 3.7 | 2.9 | 15 | 1.4 | 0.8 | 5.1 | bdl | 0.3 | 69.4 | 0.6 | – | 99.7 |
| | | | | σ | 0.1 | 0.8 | 0.9 | 4.2 | 0.8 | 0.4 | 2.7 | – | 0 | 8.7 | 0.5 | – | |
| M2442 | Wu-layer | Gl | SEM spot an | $\bar{x}$n = 5 | 0.8 | 0.6 | 1.4 | 29.7 | bdl | 22.6 | 0.5 | bdl | 0.4 | 42.2 | 0.7 | – | 98.9 |
| | | | | σ | 1 | 0.2 | 1.8 | 3 | – | 7.5 | 0.7 | – | 0.3 | 3 | 0.9 | – | |

Abbreviations: Analysis (an), Glass (Gl), Wustite (Wu), Pyroxene (Py), Loss on ignition (LOI), Total (Tot.)

local sand dunes (Howari et al., 2007), we regard their relict inclusions in slags as representing semi-molten additives from the smithing stage, in order to protect metal from hot oxidation, and not relicts of the iron ore used in the primary smelting.

The bulk composition of the Muweilah slags is provided in Table 2 (full chemical analyses are provided in *Supplementary #3*). The slags are characterized by high concentrations of FeO (60–85 wt%) and low $SiO_2$ (2.5–15 wt%) supporting their wustite-rich composition. They also have elevated concentrations of CaO (5.1–8.4 wt%) and MgO (up to 3.7 wt%), supporting the inferred use of Ca- and Mg-bearing additives.

Additionally, the ferrous artefact M2442 from Muweilah contains a thick (0.3–1.0 mm) surface layer (Fig. 8d) that, like the Muweilah smithing slags, is dominated by globular wustite and interstitial residual glass of silico-calcareous composition (Fig. 8e, Table 2). The formation of this layer must also relate to hot forging and oxidation.

### 5.2. The provenance of iron from southeastern Arabia

#### 5.2.1. Investigation of local iron ores

The ironstones and laterites collected within the U.A.E. and Oman are represented by compact and earthy masses of black and brownish colour. Their dominant ore mineral is iron hydroxide, e.g., goethite, which is supported by high loss on ignition (average = 6–12 wt%, Table 3), also recorded during heating of samples for XRF analyses in a previous study (Ploquin et al., 1999). The geochemical analyses (Table 3) reveal that some of the ore samples from Oman contain <45 wt % of $Fe_2O_3$, which is often considered insufficient for bloomery smelting, unless the ore is siderite, rich in Mn or has an easy-to-melt gangue, which does not seem to be the case for the local ores (Buchwald, 2005: 93, Rostoker and Bronson, 1990: 44–45, Stepanov et al., 2020). Overall, the closest ore occurrence to Saruq al-Hadid and Muweilah, ironstones from Jebel Faya in the U.A.E. located ~40–100 km away, was found to be sufficiently rich in iron ($Fe_2O_3 \approx 70$ wt%), and provenance investigation is therefore required to address possibility of its exploitation during the Iron Age.

#### 5.2.2. Comparison using major elements

A provenance assessment was undertaken by the multivariate comparison of SIs in ferrous objects from Saruq al-Hadid and Muweilah and iron ores, revealing several patterns (Fig. 9). Firstly, the SIs of the Saruq al-Hadid and Muweilah finished artefacts are compositionally similar to one another and comparatively homogeneous, overlapping significantly on the PCA plots and showing few outliers. The Muweilah smithing slags diverge slightly from the artefact SIs due to higher ratios of Mg and Ca in the former. Enrichment in Mg and Ca could have been influenced by the use of mafic sand rich in pyroxenes during smithing.

Secondly, the SIs of the Saruq al-Hadid and Muweilah artefacts are clearly compositionally distinct in major element concentrations from the ironstones of Jebel Faya (U.A.E.), gossans from Hilu (U.A.E.) and Lasail (Oman), and laterites from al-Russayl (Oman). This suggests that these local iron ores were not the source of the iron used in the archaeological artefacts. However, two gossan samples from Bayda (Oman) show an overlap with the analysed artefafcts. These are explored and discussed in more detail below.

Thirdly, studied sources outside southeastern Arabia, including laterites and ironstones of Saudi Arabia (Moufti, 2010), India (Borger and Widdowson, 2001; Meshram and Randive, 2011; Wimpenny et al., 2007), Iraq (Al-Bassam and Tamar-Agha, 1998), Syria (Ingo et al., 1994) and Iran (Abedini and Calagari, 2012), are largely incompatible with the composition of the iron from Saruq al-Hadid and Muweilah. This is due in most instances to the much higher contents of Al and Ti in laterites and ironstones, especially relative to contents of the other elements, although some laterites from Syria and Saudi Arabia are further differentiated by elevated contents of $P_2O_5$ (0.5–1.5 wt%, compared with <0.5 wt% $P_2O_5$ in the artefact SIs).

In terms of major element concentrations, SIs of the objects from Saruq al-Hadid and Muweilah cluster with SIs of ferrous artefacts from Luristan and some ores from the Sanandaj-Sirjan (SRJ) metallogenic belt of Iran (Mollaei et al., 2009: Table 2, Zamanian and Radmard, 2016: Table 4 and 6, Asadi and Rajabzadeh, 2014: Table 4). However, at least two SRJ ore sources (Rajabzadeh et al., 2012; Barati and Gholipoor, 2013) are geochemically different from the SIs due to higher contents of Mn and Mg relative to other elements. Furthermore, compositional variation is also revealed between different artefacts from Luristan.

Ironstones from the Levant (Jordan), although variable in composition, partly overlap with SIs from southeastern Arabian objects. Given that these ores are from the ancient iron mine of Mugharet el-Wardeh (Al-Amri, 2008), and the caravan trade between Levant/Mesopotamia and Southern Arabia is mentioned in ancient written documents (Magee, 2014: 265–266 and references therein), the provenance of ferrous objects from southeastern Arabia was further tested against this source. We compared SIs with iron smelting slags from the Iron Age site of Tell Hammeh near the Mugharet el-Wardeh mine (Veldhuijzen and Rehren, 2007; the analyses were taken from Veldhuijzen, 2005), combining the data for several trace elements (Sr, Ba, Zr, Y) with the data for major elements (Mg, Al, Si, Ca, Ti, Mn, K). The comparison of SIs against smelting slags (not ores) ameliorates the possible effects of contamination from furnace lining and charcoal during smelting. However, the PCA (Fig. 10) reveals that most slags from Tell Hammeh diverge from the SIs of southeast Arabian ferrous objects, suggesting that south Levantine iron was not used at Saruq al-Hadid and Muweilah.

#### 5.2.3. Comparison of REE distribution

The study of trace elemental trends reveals that ferrous products from southeastern Arabia are characterized by a slight enrichment of LREEs compared to HREEs, a positive to weakly negative Eu anomaly, and a weakly negative Ce anomaly (Fig. 11). At least two groups of objects can be distinguished based on the REE trends of their SIs: enriched in REEs and depleted in REEs (Fig. 11a, in red and blue respectively). One of the artefacts depleted in REEs, sample SF13024 (shown in purple in Fig. 11a), has SIs containing wustite, as well as glass and fayalite. Three other objects from Saruq al-Hadid with outlying REE trends can also be distinguished: SF13236, SF13230 and SF22529 (Fig. 11a in green, black and yellow), which suggests the use at the site of iron from different sources.

Muweilah objects generally show similar REE trends to those of

**Table 3**

Bulk XRF analyses (wt%, unless otherwise stated) of iron ores collected in the U.A.E. and Oman.

| Locality | | $Na_2O$ | MgO | $Al_2O_3$ | $SiO_2$ | $P_2O_5$ | $K_2O$ | CaO | $TiO_2$ | MnO | $Fe_2O_3$ | L.O.I. | Tot | V (ppm) | Cr (ppm) |
|---|---|---|---|---|---|---|---|---|---|---|---|---|---|---|---|
| U.A.E.; ironstones | $\bar{x}$ (n = 5) | 0.04 | 0.5 | 7.6 | 3.2 | 0.11 | 0.01 | 2.6 | 0.24 | 0.20 | 70.6 | 12.3 | 100.4 | 420 | 13519 |
| | σ | 0.01 | 0.1 | 2.0 | 1.3 | 0.02 | 0.00 | 0.8 | 0.17 | 0.09 | 4.5 | 1.5 | | 58 | 1536 |
| Oman; gossans; Bayda | OmOre-4 | 0.06 | 0.5 | 6.7 | 3.6 | 0.08 | 0.02 | 2.0 | 0.22 | 0.14 | 73.6 | 10.1 | 99.8 | 326 | 12042 |
| | OmOre-5 | 0.02 | 1.8 | 2.3 | 12.4 | 0.08 | 1.56 | 9.6 | 0.02 | 0.84 | 55.1 | 15.7 | 99.8 | 415 | 10 |
| | OmOre-6 | 0.01 | 0.4 | 0.5 | 9.0 | 0.13 | 0.07 | 16.2 | 0.02 | 0.32 | 53.7 | 19.5 | 100.1 | 211 | 10 |
| Oman, gossans; Lasail | $\bar{x}$ (n = 3) | 3.21 | 1.4 | 11.9 | 56.9 | 0.08 | 0.39 | 2.0 | 1.14 | 0.07 | 16.4 | 5.5 | 99.6 | 429 | 30 |
| | σ | 0.96 | 1.3 | 2.9 | 5.1 | 0.01 | 0.41 | 1.5 | 0.08 | 0.08 | 6.4 | 1.5 | | 224 | 26 |
| | *OmOre-32 | 1.67 | 0.5 | 5.9 | 28.0 | 0.12 | 0.13 | 1.4 | 0.77 | 0.01 | 52.1 | 7.8 | 99.2 | 1320 | 20 |
| | *OmOre-30 | 0.02 | 0.1 | 0.5 | 70.0 | 0.01 | 0.03 | 6.4 | 0.01 | 0.24 | 16.1 | 5.5 | 99.1 | 15 | 10 |
| U.A.E., gossans; Hilu | $\bar{x}$ (n = 3) | 0.14 | 0.9 | 7.3 | 24.8 | 0.06 | 0.06 | 0.7 | 0.55 | 0.21 | 56.9 | 6.6 | 100.0 | 435 | 6387 |
| | σ | 0.16 | 1.1 | 3.8 | 9.1 | 0.05 | 0.04 | 0.5 | 0.13 | 0.34 | 13.3 | 2.4 | | 96 | 10941 |
| Oman; laterites; al-Russayl | $\bar{x}$ (n = 3) | 0.23 | 2.4 | 9.8 | 25.9 | 0.02 | 0.18 | 0.4 | 0.53 | 0.84 | 46.9 | 8.8 | 99.7 | 440 | 17264 |
| | σ | 0.07 | 1.2 | 2.6 | 6.3 | 0.01 | 0.14 | 0.1 | 0.23 | 0.52 | 5.6 | 0.7 | | 243 | 7286 |
| | *OmOre-50 | 1.84 | 0.3 | 6.3 | 70.6 | 0.06 | 0.04 | 0.6 | 1.26 | 0.01 | 15.6 | 3.2 | 100.3 | 224 | 10 |
| | *OmOre-52 | 0.12 | 1.4 | 2.7 | 78.0 | 0.01 | 0.27 | 0.2 | 0.10 | 0.05 | 11.7 | 3.1 | 99.3 | 56 | 7950 |

Asterisks (*) designate outlying analyses. L.O.I. designates losses of sample mass during heating for XRF analyses. Full (major and trace element) data are provided in Supplementary #3.

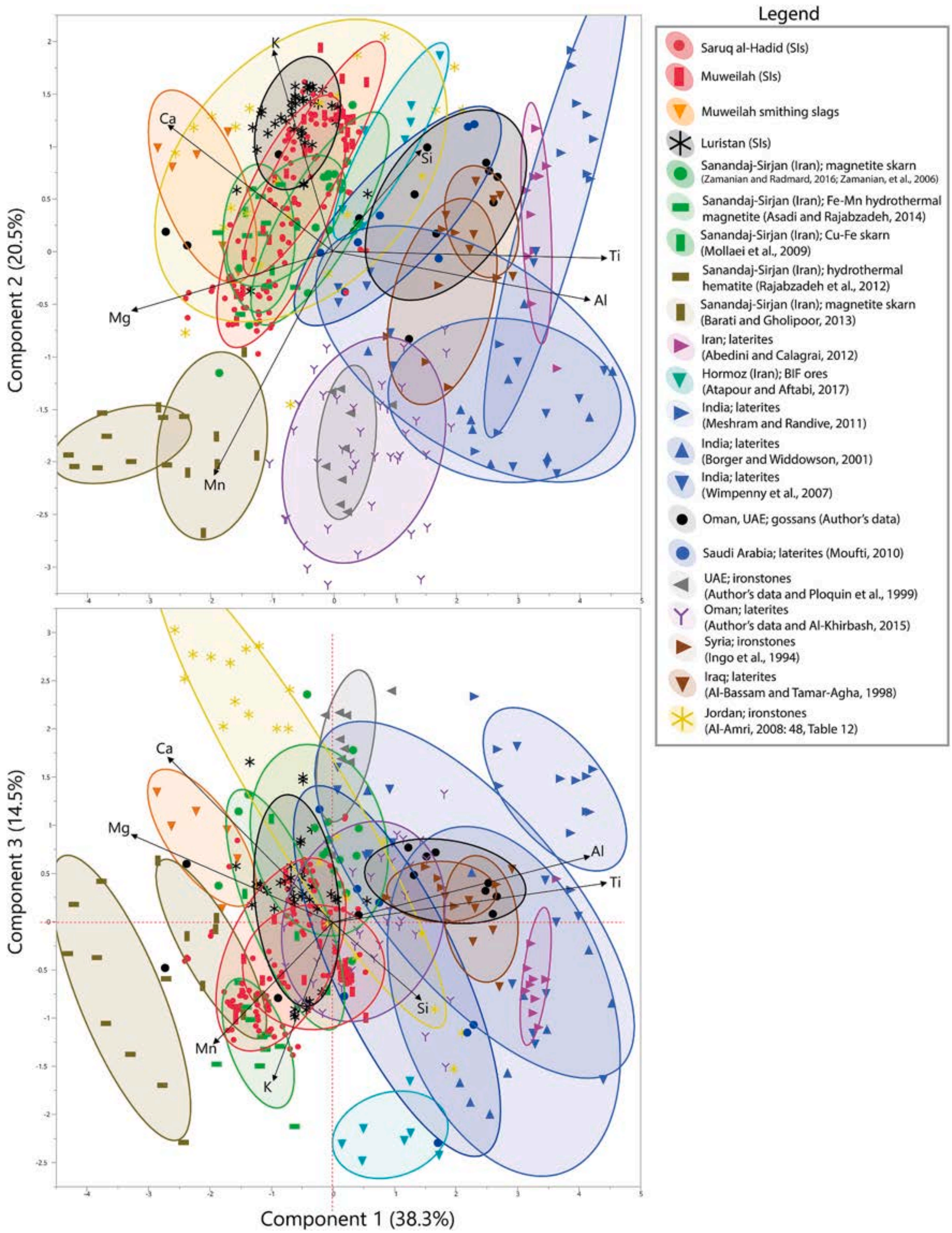


**Fig. 9.** PCA with major element oxides comparing artefacts (SIs), smithing slags and ores from Western and South Asia. Ellipses built on 75% confidence interval.

Saruq al-Hadid artefacts (Fig. 11b), with one outlying sample (M2289, shown in black). Furthermore, substantial similarities are revealed between REE distributions of SIs and smithing slags, excepting differences in Eu anomalies (positive in SIs and negative in slags), which suggest the use of similar ore sources (Fig. 11b). Eu anomalies are typically associated with the presence of plagioclase, which accumulates most of the europium, thus creating a negative anomaly in the melt (i.e., geological magma or slag melt). The plagioclase could have been originally present during geological formation of the ore body or it could have been added into the slag with sand during secondary smithing. The depletion of all trace elements in the Muweilah slags, compared to SIs, is probably due to the fact that the slags contain significant amounts of iron oxide and were analysed in bulk by ICP-MS.

In contrast to southeastern Arabian artefacts, most iron ores from the region are characterized by a flatter REE pattern, and are less enriched in HREE relative to LREEs (Fig. 12). Furthermore, most of these ores,

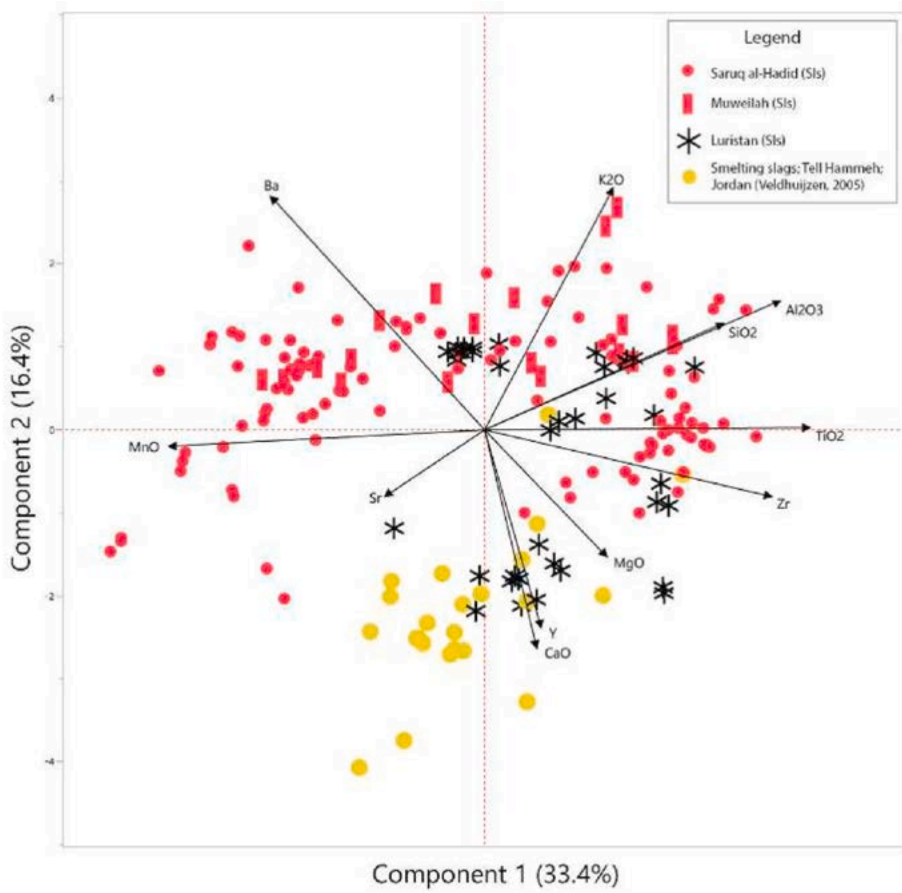


**Fig. 10.** PCA with major (Mg, Al, Si, Mn, Ti, Ca, K) and some trace elements (Sr, Zr, Ba, Y) comparing SI compositions of artefacts from Southeastern Arabia, Luristan, and iron smelting slag from the southern Levant (data from Veldhuijzen, 2005).

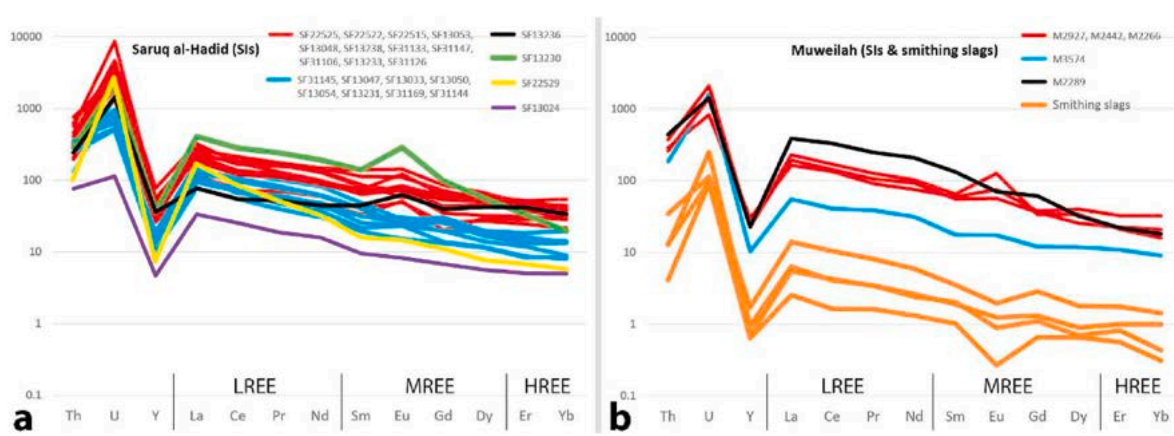


**Fig. 11.** Chondrite normalized (McDonough and Sun, 1995) spider-diagram of the distribution of trace elements in ferrous products. a. Saruq al-Hadid. b. Muweilah. Abbreviations: LREE (light REEs), MREE (medium REEs), HREE (heavy REEs).

including Bayda gossans, are also distinguished from local objects by one or several ratios including U/Y, Y/La and Th/U.

Southeastern Arabian objects reveal similar REE trends to two artefacts from Luristan, including an Iron Age II object from Bard-i-Bal (BB.17–74), and some SRJ ores, including one source of Mn ores (Zarasvandi et al., 2013) (Fig. 13, left). REE spider-grams also confirm the previous observation that some SRJ ores show a different REE pattern (Rajabzadeh et al., 2012) (Fig. 13, right). Furthermore, six Luristan objects also reveal variable REE distributions. Among other non-local ore sources, Hormoz reveals a REE pattern different from southeastern Arabian objects, while Indian laterites show a similar REE distribution, but a different Th/U ratio.

*5.2.4. Combinative comparison using major and trace elements*

Combinative comparison of major and trace elements strongly supports observations based on the separate assessment of each group of elements. In terms of negative provenance patterns, the iron ore deposits from the U.A.E. and Oman are largely discriminated from southeastern Arabian artefacts by the PCA. The U.A.E. ironstones are further identified as unlikely sources due to their high Cr concentrations (~1 wt% Cr),

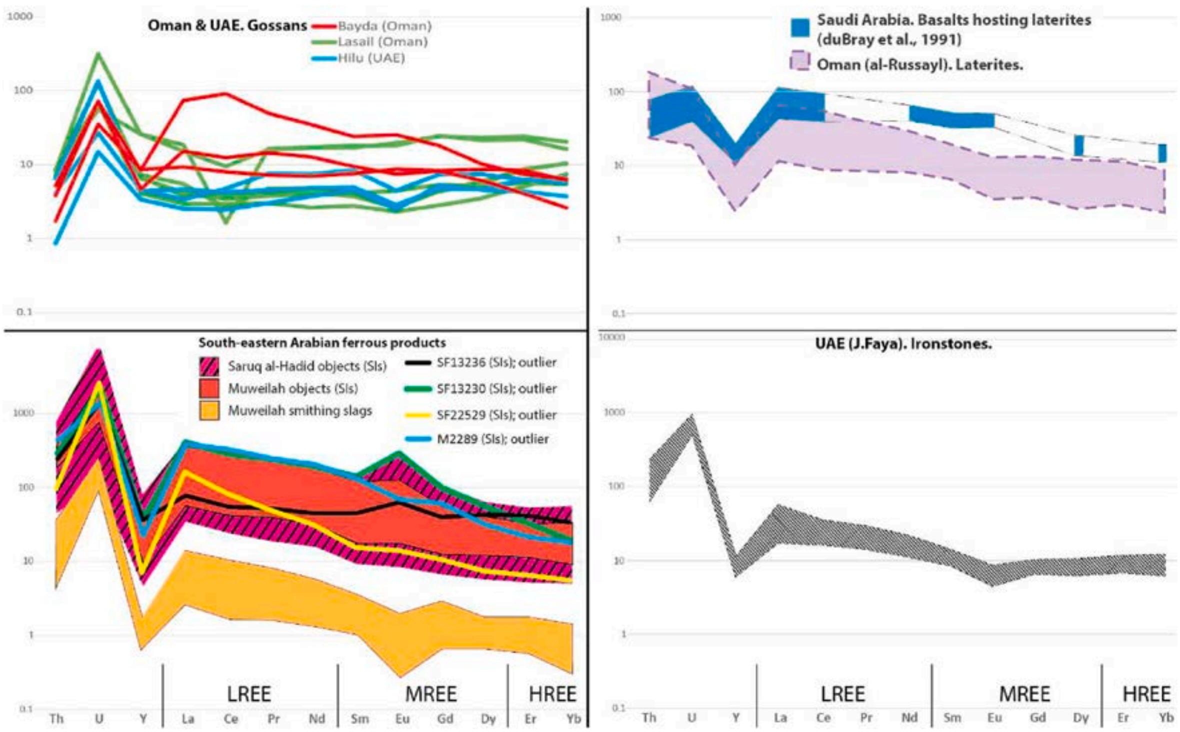


**Fig. 12.** Chondrite normalized (McDonough and Sun, 1995) spider-diagram of the distribution of trace elements in ferrous products and local iron sources.

which contrast strongly with the low Cr contents (<100 ppm) of SIs in the early Iron Age artefacts and smithing slags (*Supplementary #3*). One sample of Bayda gossan from Oman (OmOre-6, designated by arrow in Fig. 14) plots near cluster of SIs. However, this ore sample has a low iron content (16 wt% $Fe_2O_3$) and is very unlikely to have been a viable ore for iron bloomery smelting.

The local deposits therefore can be ruled out as potential sources. These conclusions are significant and, assuming that the existing data are representative of the compositional heterogeneity of their host deposits, logically powerful. The mismatch between the earliest iron from southeastern Arabia and local ore sources aligns with artefact typology and the lack of known iron slags in the region to strongly indicate a non-local provenance.

Likewise, from the broader region, the Saruq al-Hadid and Muweilah artefacts show no compositional overlap with Indian and Iranian laterites, and only limited overlap with iron ores from Hormoz Island, which is the most proximate Iranian source to southeastern Arabia (Fig. 14). After eliminating some of the outlying ore sources (Figs. 15 and 16), it becomes clearer that a number of artefacts from southeastern Arabia cluster together with three objects from Luristan (BB.17–74, SK.68/19_9, WKA.59–9_5) and the Baba Ali magnetite skarn deposit from the SRJ (Zamanian and Radmard, 2016; Zamanian et al., 2007). This possible provenance is indirectly supported by the fact that many of the analysed objects, including some outliers (e.g., SF13236 designated in Fig. 15) contain SIs with high or elevated contents of CaO (6–15 wt%) and MgO (3–5 wt%). These elements are typically enriched in skarns, which are widespread in the SRJ (Ghorbani, 2013: 90–91).

Two other SRJ deposits – Mn ores and Fe–Mn hyrothermal magnetite – remained after elimination of some ore sources, and show limited overlap with the analysed ferrous objects (Figs. 15 and 16). Manganese ores appear, in general, to have been used only rarely for ancient iron production. In contrast, Fe–Mn hydrothermal ores (Asadi and Rajabzadeh, 2014), clustering together with artefacts SF31144 and SF22529, could have been exploited in ancient Iran since SIs from many other analysed artefacts from Saruq al-Hadid contain elevated MnO contents (1–5 wt%).

The three remaining artefacts from Luristan (WK.A10-20_6–11, WK.A10-20_6–5, GG.71/80_10) diverge to varying extents from the rest of the analyses, indicating a different composition and different ore source (s). This may reflect the fact that the Luristan artefacts incorporated in our study are mostly from the Iron Age III period (800-600 BCE), when iron prospection, exploitation, production and trade had probably intensified compared to preceding periods.

The SIs formerly identified as depleted in REE (Figs. 15 and 16, shown in blue) are discriminated from the other artefacts on the PCA and hierarchical cluster analysis, confirming their different composition. The Muweilah artefact M3854 and Muweilah smithing slags also cluster with some of these samples and therefore may have a common provenance. The cause for REE depletion in SIs of this group (not considering smithing slags), is most likely related to the composition of the parent ore(s), since most of SIs are composed of glass and fayalite, without wustite (i.e., alternative cause for REE depletion).

Other than M2289, all objects from Muweilah plot alongside objects from Saruq al-Hadid, indicating common provenance for the iron used at both sites. In contrast, the Muweilah outlier M2289, together with banded iron formations (BIF) from Hormoz (comprising cluster 5 in Figs. 15 and 16), is discriminated from the other objects. The possible derivation of M2289 from Hormoz is unexpected. According to Killick (2014), BIFs were rarely exploited in prehistory unless strongly weathered. On Hormoz, beds of red ochrous ores up to several metres thick were formed by the weathering of BIFs and were mined in the past as a mineral dye (Hassanlouei and Rajabzadeh, 2019). Although the iron content of these ochrous ores can be sufficiently high for bloomery smelting, no traces of iron slag have been reported from the island and the first mention of Hormoz iron ores in ancient texts occurs after the 13th Century CE (Allan, 1979: 67). The question of bloomery smelting of Hormoz iron deposits therefore deserves further exploration.

### 5.2.5. Summary of the provenance investigation

While the compositional parallels with the Baba Ali magnetite skarn deposit (Zamanian and Radmard, 2016) are indicative of a possible provenance for a majority of the iron objects, iron ores and deposits of similar type and in some cases with similar compositions occur at multiple locations along the SRJ metamorphic belt from northwestern to

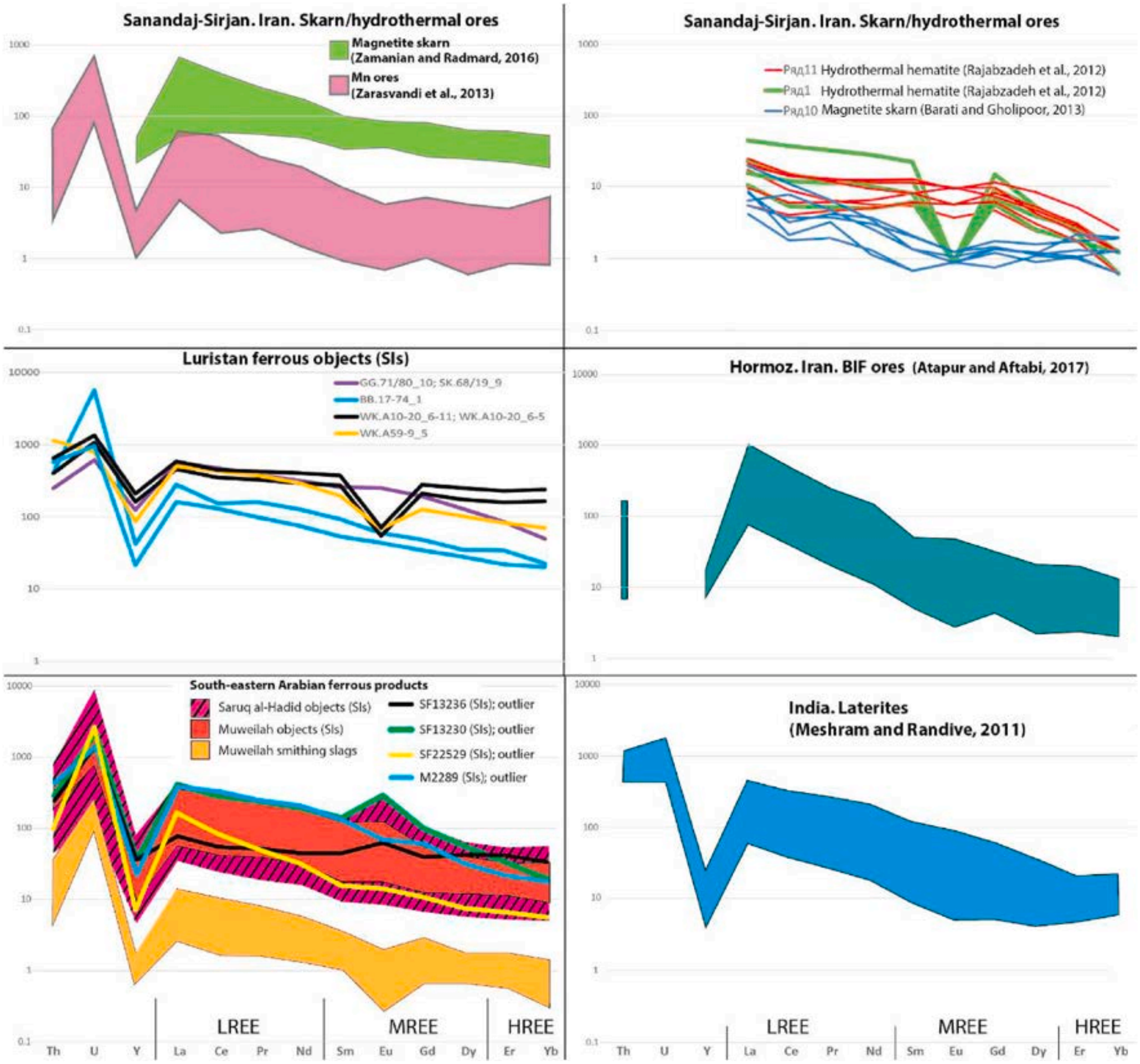


**Fig. 13.** Chondrite normalized (McDonough and Sun, 1995) spider-diagram of distribution of trace elements in local ferrous products and non-local iron objects (SIs) and sources.

southeastern Iran, several of which have evidence for past exploitation (Fig. 3) (Nabatian et al., 2015). Although this situation complicates sourcing studies, a more precise delineation of provenance for the analysed objects may eventually be possible given the availability of additional compositional and isotopic data (e.g. Brauns et al., 2020) from other SRJ ore deposits and for more early iron objects from northwestern and southeastern Iran.

Despite these uncertainties, the parallels in both artefact typologies and specific forging techniques identified between iron artefacts from Saruq al-Hadid and Luristan reinforce the provenance hypotheses generated from the compositional data. Together, these highlight the historically-exploited mines of the western Zagros – Shamsabad, Ahangaran or Khugan – and neighbouring archaeological sites as the most probable locations for the smelting and forging of the finished iron objects from early Iron Age southeastern Arabia, particularly Saruq al-Hadid. Further analyses of these putative sources are needed to compare their composition against ferrous artefacts and other ores to better address questions of provenance.

## 6. Discussion

The results of the archaeometric analyses, although preliminary, suggest that the ferrous objects from two early Iron Age sites in southeastern Arabia, Saruq al-Hadid and Muweilah, were not smelted from locally available iron resources. Instead, most appear to have been imported – at least in some instances as complete, finished objects (based on similarities in fabrication techniques; Stepanov et al., 2019b) – from more than 1000 km away in the western Zagros of Iran, where the iron was both smelted and forged.

These findings support a range of other material parallels known to exist between southeastern Arabia and western Iran – the typology of bronze swords, bridge-spouted pottery, columned building architecture, as well as the geochemical analyses of bitumen (Overlaet, 2003: 152–166, Potts, 2012, Magee, 2005, 2010, Velde, 2003, Van de Velde et al., 2017) – most of which first emerged during the Late Bronze Age, but became much more prominent during the early Iron Age (Potts, 2012: 97). However, archaeometric studies indicate that some typologically "Iranian" artefacts from early Iron Age southeastern Arabia were in fact manufactured from local Arabian resources (Prange and Hauptmann, 2001; Benoist and Méry, 2012; Potts, 2012: 97; Gernez, 2018). As Gernez (2018: 172) notes, although the chronological primacy of some of these artefact prototypes in Iran is clear, "it is difficult to precisely quantify and qualify the impact of Iranian crafts on Arabian ones", and southeastern Arabian technologies and typologies quickly

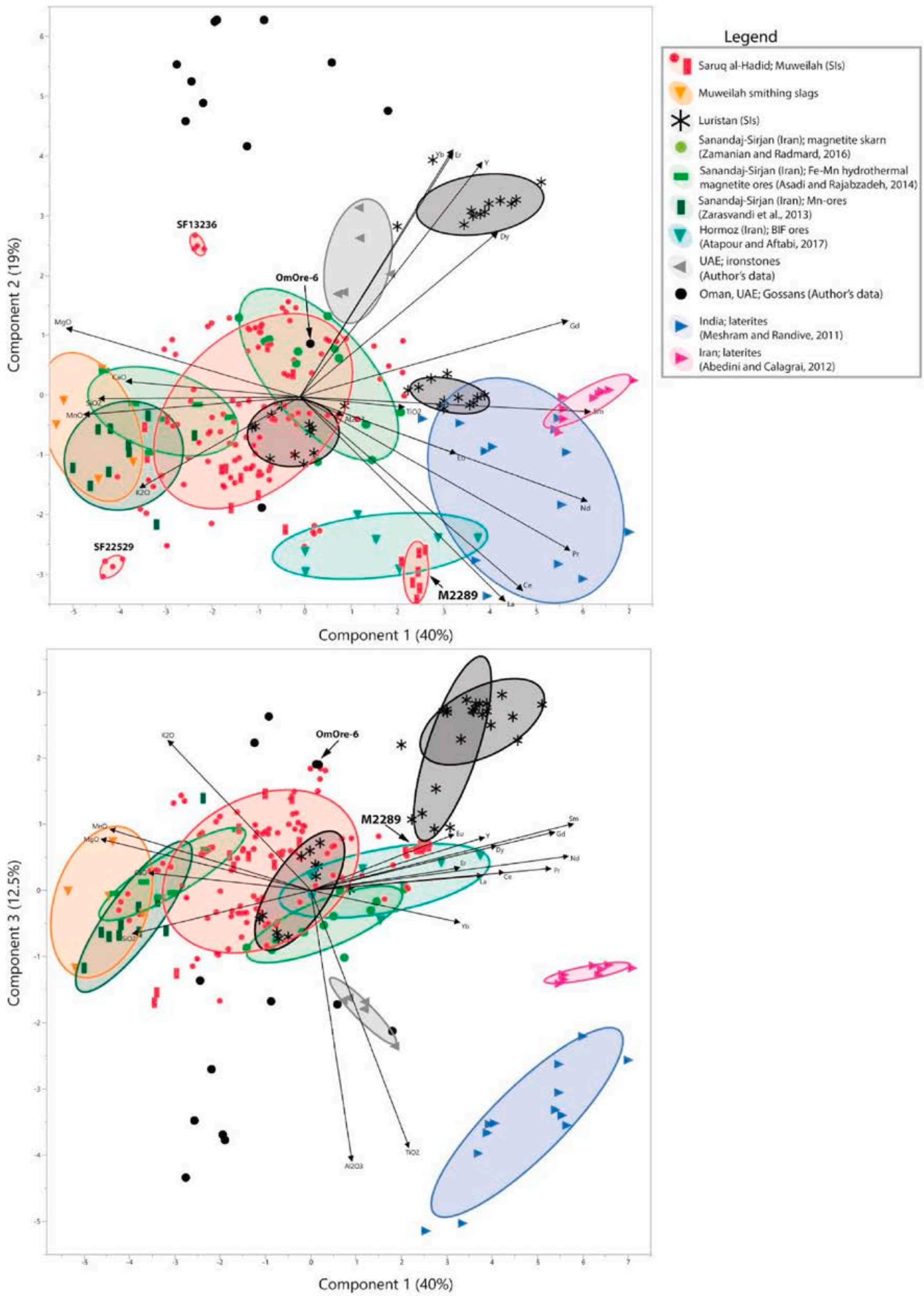


**Fig. 14.** PCA plots of major (Mg, Al, Si, Mn, Ti, Ca, K) and trace (Y, REEs) elements comparing SIs, slags and ores. Several outlying analyses of ores and SIs are designated on the plot. Ellipses were built on 75% confidence interval.

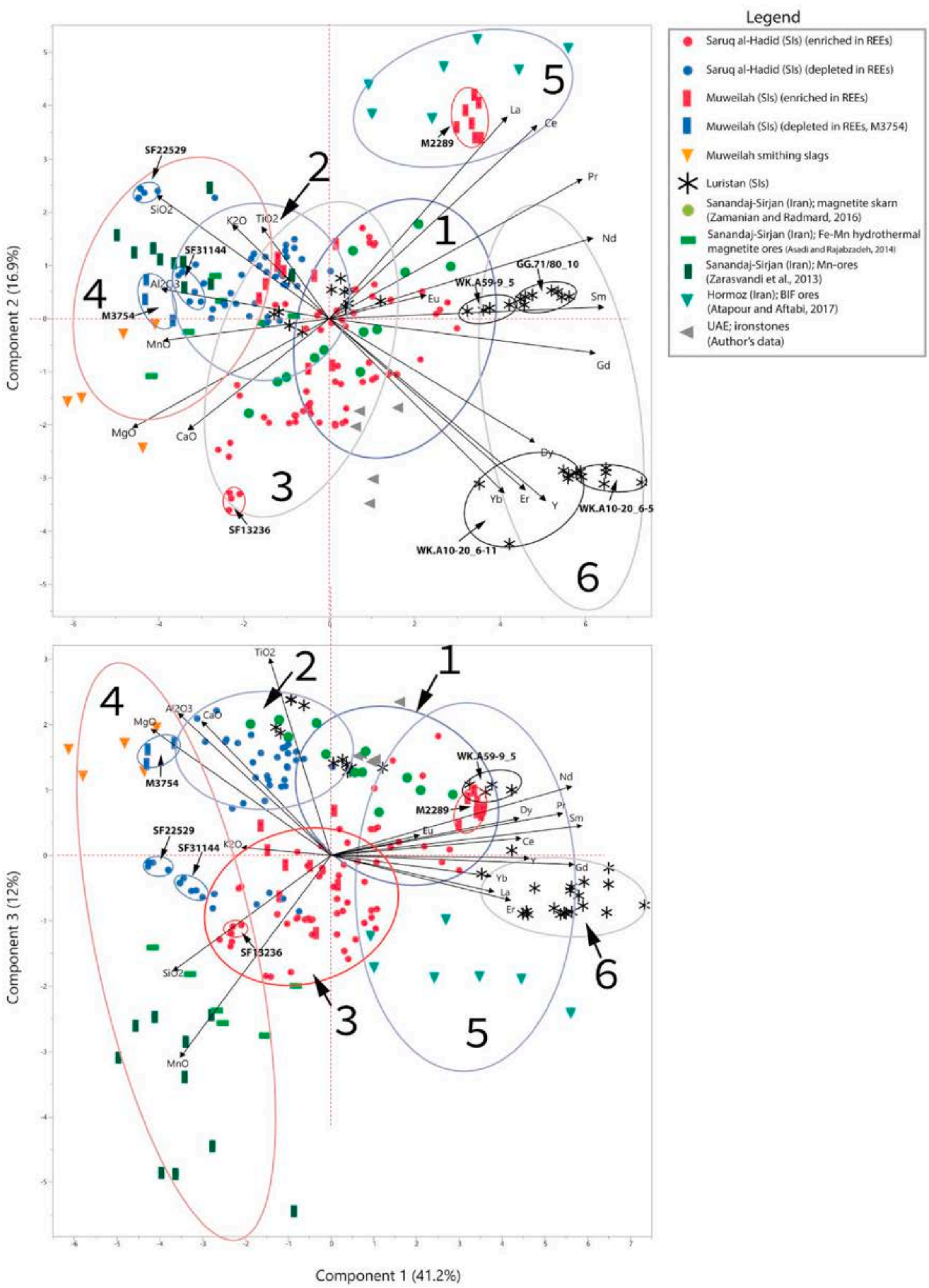


**Fig. 15.** PCA plot of major and trace elements, after elimination some of the ore sources outlying in PCA from Fig. 14. Six designated ellipses represent hierarchically distinguished clusters (see Fig. 16). Analyses of artefacts-outliers are designated on the plot. Ellipses built on 90% confidence interval.

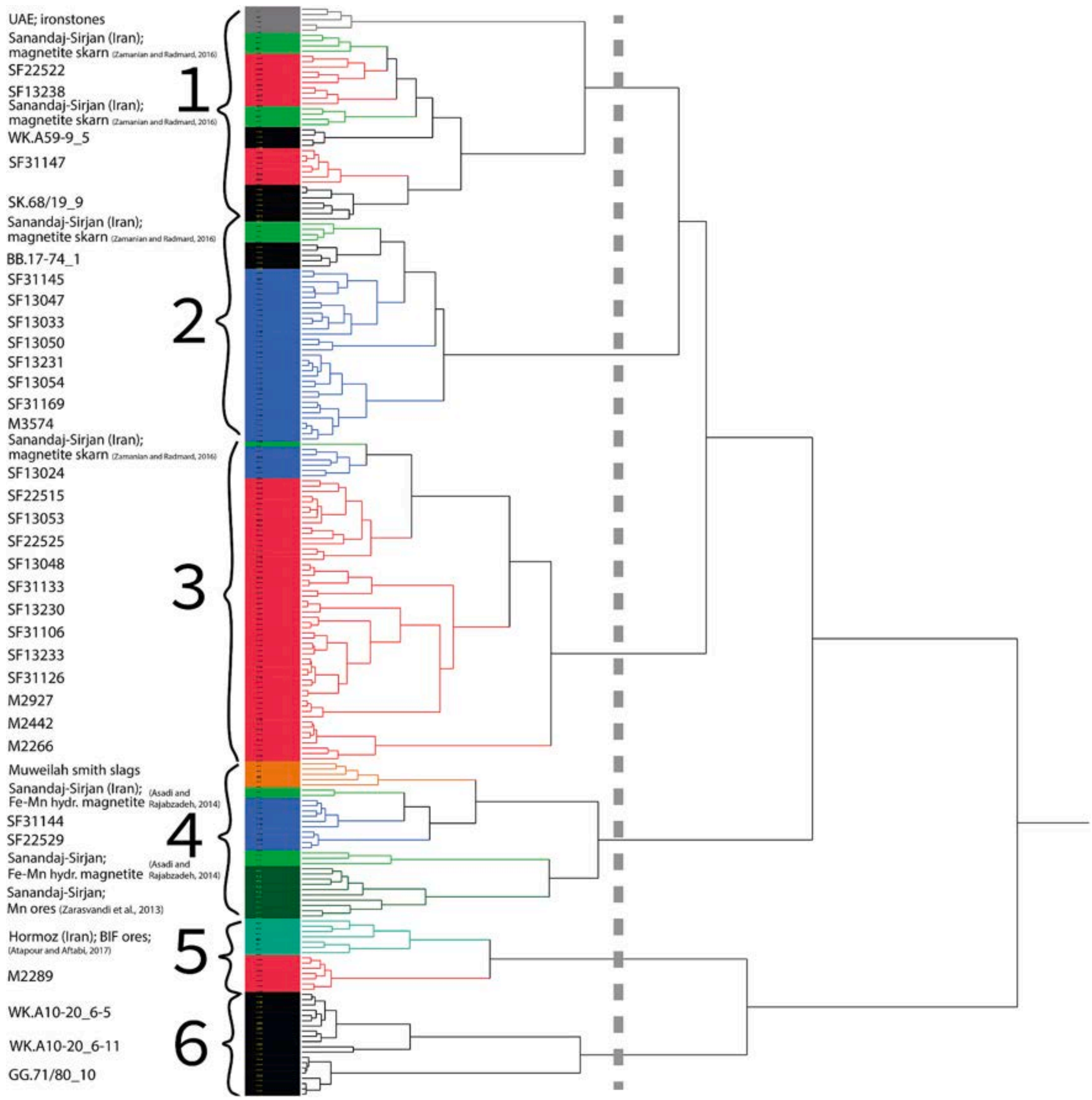


**Fig. 16.** Hierarchical clustering tree for the dataset presented in Fig. 15. Performed by Ward's method.

developed along local, culturally-specific lines. Thus, archaeometric studies both enhance and complicate our understanding of the possible vectors of cultural influence between western Iran and southeastern Arabia in the late second and early first millennia BCE.

Southeastern Iran remains a proximate and thus possible source of imports of iron into southeastern Arabia, based on the presence of major local iron ore sources displaying ancient workings (Abbasnejad Seresti, 2009). However, large-scale imports of iron from southeastern Iran seem unlikely given the fact that the area is apparently sparsely populated at this time. Moreover, the known ferrous assemblages from Tepe Yahya postdate 800 BCE, after the peak period of activities at Saruq al-Hadid and, to a lesser extent, Muweilah (Magee et al., 2004: 77–81).

Material parallels with other iron producing and using regions neighbouring southeastern Arabia are less pronounced in the archaeological record but deserve further consideration, particularly in relation to the Levant and northern Mesopotamia. The few relevant Assyrian historical sources referring to the Persian Gulf indicate that significant direct interactions between these regions began with the reign of Sargon II (721–705 BCE, Potts, 2009a; Potts, 1985), largely postdating the peak of iron use at Saruq al-Hadid and Muweilah. However, such historical sources are rare and lacunae can be easily over-interpreted; indeed, material with stylistic and typological parallels to the Neo-Assyrian world is known from Saruq al-Hadid and other sites in southeastern Arabia (e.g., Potts, 2009b; Weeks et al., 2019b). Significantly, this material may well have arrived via indirect contacts. Magee (2014: 265–266), for example, suggests that Syrian iron may have been used in Iron Age Arabia, based on historical evidence that iron was a commodity traded by south Arabian camel caravaneers in the eighth century BCE. A variety of material remains from Saruq al-Hadid and Muweilah – particularly scarabs of Egyptian or "Egyptianising" nature (Boraik, 2017; cf. Sperveslage, 2016), a sherd with incised South Arabian letters (Magee, 1999), and a decorated shell disc from Saruq al-Hadid with a close match at Tayma in northwestern Arabia (Weeks et al., 2019b) – support the idea of connections with west Arabian overland trade routes and thus indirect access to the material products of the Levant and Syria.

Significantly, however, the archaeometric and typological analyses presented here do not support the idea that early southeastern Arabian iron came from greater northern Mesopotamia. Key iron sources from this region – the Kerry ore source of Syria, Mugharet el-Wardeh in Jordan, and the Hussainiyat source from Iraq – mostly differ in their major and trace element signatures in comparison to iron objects from southeastern Arabia.

With few exceptions (e.g., Curtis, 2013; Rabinovich et al., 2019), the typology of early Iron Age iron objects from Greater Mesopotamia is neither sufficiently distinct or well known to contribute to the discussion of provenance, partly due to the poor preservation of ancient iron. Iron swords with flanged hilts of the type recorded in southeastern Arabia and western Iran are not known from the Levant and are rare in Mesopotamia, with the only known examples coming from Nimrud (Pleiner and Bjorkman, 1974: Fig. 2.1). Thus, while it is possible that some of the southeastern Arabian iron objects were fabricated in the urbanized centres of northern Mesopotamia, the available evidence does not support this hypothesis.

Likewise, it has not been possible to archaeometrically identify the use of Indian iron in early Iron Age southeastern Arabia, despite the existence of developed iron production in South Asia at this time. Although there is abundant evidence for contact between Arabia and South Asia in the subsequent Late Pre-Islamic period and historical sources indicate the trade of Indian iron (alongside iron from other sources) in the western Indian Ocean at this time (Delrue, 2008: 90–91), such exchange relations do not appear to have been as intense five or six centuries earlier. More generally, these observations highlight the significant chronological gap between the current evidence for iron use in southeastern Arabia in the Iron Age and the subsequent Late Pre-Islamic period. This gap, covering perhaps two centuries (Delrue, 2008: 386–387), makes any attempt to describe a local developmental sequence for iron production and use speculative.

Nevertheless, the results presented here facilitate a better understanding of the possible role of Saruq al-Hadid in early Iron Age southeastern Arabia. The similar SI compositions of ferrous objects from Saruq al-Hadid and the majority of objects from Muweilah, as well as several ceramic parallels, indicate that the sites participated in the same exchange networks. However, the fact that Saruq al-Hadid contains the vast majority of iron objects known from the region suggests that the site may have been a key node in their long distance movement. The compositional variability of the iron objects from Saruq al-Hadid highlights its role as a site for the collection and deposition of material from a wide variety of sources, a pattern that can be observed not only for iron but also a range of other materials (Weeks et al., 2019a; Karacic et al., 2018b).

Finally, despite the fact that iron smelting was unlikely to have taken place in southeastern Arabia during the early Iron Age, the archaeometric identification of smithing slags and semi-products from Muweilah presented here provides the first conclusive evidence for local iron smithing activities at this time. At Muweilah, these activities could have focused on the forging of semi-finished ferrous products (ingots, billets, blooms, etc.) and/or the re-forging of finished objects. Such small smithies may also have existed at other Iron Age settlements in the region, although the evidence to support this hypothesis is lacking. The influx and circulation of foreign iron objects in southeastern Arabia would have created a pool of metal artefacts eventually requiring repair, including forge-welding. This would have been a less technologically sophisticated and innovative operation than the smelting of iron ores, and might feasibly have been carried out by local bronze- or iron-smiths.

## 7. Conclusions

The present study, through the application of an integrated programme of archaeometric analyses of specimens from southeastern Arabia and adjacent regions, provides the first scientific evidence supporting the long distance import of iron objects from the western Zagros to southeastern Arabia in the late second and early first millennium BCE. These findings support well known parallels in material culture between the western Zagros and southeastern Arabia that nevertheless remain difficult to relate to cultural or economic ties with specific regions. The use of iron from the Levant and/or northern Mesopotamia in early Iron Age southeastern Arabia seems unlikely, based on the currently available analytical evidence. However, this area remains a tantalising prospect based on limited archaeological and historical evidence; more iron ores and metallurgical residues from these areas will need to be analysed in order to arrive at definitive conclusions on the matter. Overall, the results of the present study provide a new perspective on socio-cultural and economic change in southeastern Arabia during the apogee of the local Iron Age, and highlight the role of the region's interactions with wider Western Asia in these developments.

## Declaration of competing interest

None.

## Acknowledgments

This research was supported by the Dubai Municipality (contract 639/1/1413904) and the University of New England, Australia (through the provision of an international PhD studentship to the lead author). We acknowledge both organisations for their financial and logistical support. Additionally, we express our great appreciation to: staff of Dubai Municipality and Dr. Hussein Qandil for their help and permission to study samples from Saruq al-Hadid; Professor Peter Magee (Bryn Mawr College), Dr. Sabah Jasim and Dr. Eisa Yousif (Sharjah Archaeological Museum), and Ms. Hazelle Anne Page for permission to sample and study Muweilah artefacts; Sultan al-Bakri (Ministry of Culture and Heritage, Sultanate of Oman) for permission to sample Omani iron ores; Dr. Dennys Frenez and the late Professor Maurizio Tosi for their assistance during field work in Oman; Dr. Philippe Dillmann for advice regarding statistical approaches; Dr. Rosanna Murphy for help with LA-ICP-MS; and Dr. Steve Karacic for information regarding the Muweilah artefacts. We further thank Dr. Derek Kennet, Dr. Mark Händel, Dr. Luke Milan, Dr. James Roberts, Dr. Gary Marriner, Ms.Emma Watt, Dr. Claire Newton, Mr. Malcom Lambert, Ms. Hélène David-Cuny, Ms. Kim Newman, and Mr. John Pesor for help and advice received during the work. Finally, we thank the two anonymous reviewers whose feedback helped to improve the quality of the paper.

## Appendix A. Supplementary data

Supplementary data to this article can be found online at https://doi.org/10.1016/j.jas.2020.105192.

## References

Abedini, A., Calagari, A., 2012. The mineralogy and geochemistry of Permian lateritic ores in east of Shahindezh, West-Azarbaidjan province. Iran. J. Crystallogr. Mineral. 20, 59–72.

Abbasnejad Seresti, R., 2009. Iron archaeometallurgy in the triangle of the Sirdjan, Neiriz and Shahr-e-Babak. Int. J. Humanit. 16 (1), 1–16.

Abdulhay, G.J., Zahrani, Al, 2005. A.M., Al shihri, M. In: Industrial Minerals Map of the Kingdom of Saudi Arabia, Scale 1:4,000,000. Kingdom of Saudi Arabia, Jeddah.

Allan, J.W., 1979. Persian Metal Technology: 700–1300 AD. Ithaca Press, Oxford.

Aitchison, J., 1986. The statistical analysis of compositional data. Chapman & Hall, London.

Al-Amri, Y.A., 2008. The Role of the Iron Ore Deposit of Mugharet El-Wardeh/Jordan in the Development of the Use of Iron in Southern Bilad El-Sham. PhD Thesis. Bochum University, Germany.

Al-Bassam, K.S., Tamar-Agha, M., 1998. Genesis of the Hussainiyat ironstone deposit, western Desert. Iraq. Miner. Deposita 33 (3), 266–282.

Al-Bassam, K.S., Hak, J., 2006. Metallic and industrial rocks and minerals. In: Jassim, S. Z., Goff, J.C. (Eds.), Geology of Iraq. Dolin, Prague, pp. 288–302.

Al-Khirbash, S., 2015. Genesis and mineralogical classification of Ni-laterites, Oman Mountains. Ore Geol. Rev. 65, 199–212.

Al-Khirbash, S., Semhi, K., 2018. 2018. Origin of Late Cretaceous ironstones deposits, northern Oman Mountains, Oman: REE geochemistry approach, in: 20th EGU General Assembly, EGU2018. In: Proceedings from the Conference Held 4-13 April, 2018 in Vienna, Austria, p. 2095.

Al-Khraysheh, F., An-Nashef, K., 2007. Dubai: civilization and progress throughout three thousand years. In: Five Seasons of Joint Archaeological Excavations between the Emirate of Dubai and the Hashemite Kingdom of Jordan at Saruq Al Hadid. Commerce and Tourism Department, Government of Dubai (in Arabic), Dubai.

Anaf, W., 2010. Study on the formation of heterogeneous structures in leached layers during the corrosion process of glass, CeROArt. Conservation, Exposition, Restauration d'Objets d'Art, Association CeROArt asbl. https://doi.org/10.4000/ceroart.1561.

Antonini de Maigret, S., Robin, C.J., 2015. Two silver vases of Greco-Roman style from the 'treasure of wādī Ḍura' (Yemen). In: Arbach, M., Schiettecatte, J. (Eds.), Pre-Islamic South Arabia and its Neighbours: New Developments of Research. Proceedings of the 17th Rencontres Sabéennes Held in Paris, 6–8 June 2013. Archaeopress, Oxford, pp. 3–12.

Asadi, S., Rajabzadeh, M.A., 2014. Geochemistry, paragenesis, and wall-rock alteration of the qatruyeh iron deposits, southwest of Iran: implications for a hydrothermal-metasomatic genetic model. J. Geol. Res. https://doi.org/10.1155/2014/590540.

Atapour, H., Aftabi, A., 2017. The possible synglaciogenic Ediacaran hematitic banded iron salt formation (BISF) at Hormuz Island, southern Iran: implications for a new style of exhalative hydrothermal iron-salt system. Ore Geol. Rev. 89, 70–95.

Barati, M., Gholipoor, M., 2013. Mineralogy, geochemistry and origin of Zafarabad iron deposit based on REE and trace elements of magnetite. Econ. Geol. 235–254.

Bauvais, S., Fluzin, P., 2009. Archaeological and archeometrical approaches of the chaîne opératoire in iron and steelmaking: methodology for a regional evolution study. In: Roux, V., Rosen, S. (Eds.), Techniques and People: anthropological perspectives on technology in the archaeology of the proto-historic and early historic periods in the southern Levant. Mémoires et Travaux, De Boccard, pp. 157–178.

Barton, M.D., 2013. Iron oxide (-Cu-Au-REE-P-Ag-U-Co) systems. In: Turekian, K, Holland, H (Eds.), Treatise on Geochemistry, 2nd. Elsevier Science, pp. 515–541.

Bauvais, S., Berranger, M., Boukezzoula, M., Leroy, S., Disser, A., Vega, E., Aubert, M., Dillmann, P., Fluzin, P., 2018. 'Guard the good deposit': technology, provenance and dating of bipyramidal iron semi-products of the durrenentzen deposit (Haut-Rhin, France). Archaeometry 60, 290–307.

Bayley, J., Dungworth, D., Paynter, S., 2001. Archaeometallurgy. English Heritage, London.

Belli, O., 1991. Ore Deposits and mining in Eastern Anatolia in the Urartian period: silver, copper and iron. In: Merhav, R. (Ed.), Urartu A Metalworking Center in the Frist Millennium BCE. Israel museum, Jerusalem, pp. 16–41.

Benoist, A., 2007. An Iron Age II snake cult in the Oman peninsula: evidence from Bithnah (Emirate of Fujairah). Arabian Archaeol. Epigr. 18, 34–54.

Benoist, A., Méry, S., 2012. Initial results from the programme of petrographic analysis of Iron Age pottery from the United Arab Emirates. Arabian Archaeol. Epigr. 23, 70–91.

Benoist, A., Le Carlier, C., Goy, J., Degli Esposti, M., Armbruster, B., Attaelmanan, G., 2015. Snake, copper and water in southeastern Arabian religion during the Iron Age: the Bithnah and Masafi evidence. In: Arbach, M., Schiettecatte, J. (Eds.), Pre-Islamic South Arabia and its Neighbours: New Developments of Research, Proceedings of the 17th Rencontres Sabéennes Held in Paris. BAR. Archaeopress, Oxford, pp. 6–8.

Biggs, L., Bellina, B., Martinón-Torres, M., Pryce, T.O., 2013. Prehistoric iron production technologies in the Upper Thai-Malay Peninsula: metallography and slag inclusion analyses of iron artefacts from Khao Sam Kaeo and Phu Khao Thong. Archaeol. Anthropol. Sci. 5 (4), 311–329.

Boraik, M., 2017. Seals from Saruq Al-Hadid Archaeological Site. Dubai Municipality (in Arabic), Dubai.

Borger, H., Widdowson, M., 2001. Indian laterites, and lateritious residues of southern Germany: a petrographic, mineralogical, and geochemical comparison. Z. Geomorphol. 45 (2), 177–200.

Brauns, M., Yahalom-Mack, N., Stepanov, I., Sauder, S., Keen, J., Eliyahu-Behar, A., 2020. Osmium Isotope Analysis as an Innovative Tool for Provenancing Ancient Iron: A Systematic Approach. Plos One 15 (3). https://doi.org/10.1371/journal.pone.0229623.

Buchwald, V.F., Wivel, H., 1998. Slag analysis as a method for the characterization and provenancing of ancient iron objects. Mater. Char. 40, 73–96.

Buchwald, V.F., 2005. Iron and steel in ancient times. Kgl. Danske Videnskabernes Selskab, Copenhagen.

Carter, E., Deaver, K., 1996. Excavations at Anshan (Tal-E Malyan): the Middle Elamite Period, vol. 2. The University Museum, Philadelphia.

Chakrabarti, D.K., 1992. The Early Use of Iron in India. University Press, Oxford.

Charlton, M.F., Crew, P., Rehren, T., Shennan, S.J., 2010. Explaining the evolution of ironmaking recipes–An example from northwest Wales. J. Anthropol. Archaeol. 29, 352–367.

Charlton, M.F., Blakelock, E., Martinón-Torres, M., Young, T., 2012. Investigating the production provenance of iron artifacts with multivariate methods. J. Archaeol. Sci. 39, 2280–2293.

Charlton, M.F., 2015. The last frontier in 'sourcing': the hopes, constraints and future for iron provenance research,. J. Archaeol. Sci. 56, 210–220.

Condoluci, C., 2018. The Iron Age architecture of Husn Salut. In: Avanzini, A., Esposti, D. E. (Eds.), Husn Salut and the Iron Age of South East Arabia. L'Erma di Bretschneider, Rome, pp. 201–278.

Curtis, J., 2013. An Examination of Late Assyrian Metalwork. Oxbow Books, Oxford.

Crew, P., 2000. The influence of clay and charcoal ash on bloomery slags. Il ferro nelle Alpi 38–47.

Delrue, P., 2008. Archaeometallurgical Analyses of Pre-islamic Artefacts from Ed-Dur (Emirate of Umm Al-Qaiwain, U.A.E.). PhD Thesis. Ghent University.

Desaulty, A.-M., Mariet, C., Dillmann, P., Joron, J.L., Fluzin, P., 2008. A provenance study of iron archaeological artefacts by Inductively Coupled Plasma-Mass Spectrometry multi-elemental analysis. Spectrochim. Acta B: Atom. Spectros. 63, 1253–1262.

Desaulty, A.-M., Dillmann, P., L'Héritiera, M., Mariet, C., Gratuze, B., Joron, J.-L., Fluzin, P., 2009. Does it come from the Pays de Bray? Examination of an origin hypothesis for the ferrous reinforcements used in French medieval churches using major and trace element analyses. J. Archaeol. Sci. 36, 2445–2462.

Dillmann, P., L'Héritier, M., 2007. Slag inclusion analyses for studying ferrous alloys employed in French medieval buildings: supply of materials and diffusion of smelting processes. J. Archaeol. Sci. 34, 1810–1823. https://doi.org/10.1016/j.jas.2006.12.022.

Dillmann, P., Schwab, R., Bauvais, S., Brauns, M., Disser, A., Leroy, S., Gassmann, G., Fluzin, P., 2017. Circulation of iron products in the North-Alpine area during the end of the first Iron Age (6th-5th c. BC): a combination of chemical and isotopic approaches,. J. Archaeol. Sci. 87, 108–124. https://doi.org/10.1016/j.jas.2017.10.002.

Disser, A., Dillmann, P., Leroy, M., L'Héritier, M., Bauvais, S., Fluzin, P., 2017. Iron supply for the building of Metz cathedral: new methodological development for provenance studies and historical considerations. Archaeometry 59 (3), 1–18. https://doi.org/10.1111/arcm.12265.

Dostal, W., 2002. The Austrian-Saudi Arabian collaborative project in the south-western region of the Kingdom of Saudi Arabia. A preliminary report. Proceed. Seminar Arabian Stud. 32, 225–232.

duBray, E.A., Stoeser, D.B., McKee, E.H., 1991. Age and petrology of the Tertiary as Sarat volcanic field, southwestern Saudi Arabia. Tectonophysics 198 (2-4), 155–180.

Dungworth, D., Wilkes, R., 2007. An investigation of hammerscale. Hist. Metall. 43, 33–46.

Dunster, J., Dungworth, D., 2012. Blacksmiths' Fuel the Analysis of Slags from Archaeological and Contemporary Iron-Working, Technology Report. English Heritage, Portsmouth.

Dussubieux, L., Robertshaw, P., Glascock, M.D., 2009. LA-ICP-MS analysis of African glass beads: laboratory inter-comparison with an emphasis on the impact of corrosion on data interpretation. Int. J. Mass Spectrom. 284, 152–161.

Edgell, H.S., 2006. Arabian Deserts: Nature, Origin and Evolution. Springer, The Netherlands.

Eekelers, K., Degryse, P., Muchez, P., 2016. Petrographic investigation of smithing slag of the Hellenistic to Byzantine city of Sagalassos (SW-Turkey). Am. Mineral. 101 (5), 1072–1083.

Erb-Satullo, N.L., 2019. The innovation and adoption of iron in the ancient Near East. J. Archaeol. Res. 27, 557–560. https://doi.org/10.1007/s10814-019-09129-6.

Gernez, G., 2018. 'Uqdat al-Bakrah in the context of eastern Arabia and the ancient Near Eastern archaeology. In: Yule, P., Gernez, G. (Eds.), Early Iron Age Metal-Working Workshop in the Empty Quarter, Al-Zobira Province, Sultanate of Oman. Verlag Dr. Rudolf Habelt GmbH, Bonn, pp. 171–177.

Gernez, G., Benoist, A., Jean, M., 2017. The Iron Age in adam the discovery of a ritual complex near Jabal Mudmahr. In: Gernez, G., Giraud, J. (Eds.), Taming the Great Desert. Adam in the Prehistory of Oman. Ministry of Heritage and Culture, Sultanate of Oman, pp. 49–80.

Ghorbani, M, 2013. In: The economic geology of Iran. Mineral Deposits and Natural Resources. Springer Science, Dordrecht.

Gordon, R.B., Van Der Merwe, N., 1984. Metallographic study of iron artefacts from the eastern Transvaal, South Africa. Archaeometry 26, 108–127.

Hassanlouei, B.T., Rajabzadeh, M.A., 2019. Iron ore deposits associated with Hormuz evaporitic series in Hormuz and Pohl salt diapirs, Hormuzgan province, southern Iran. J. Asian Earth Sci. 172, 30–55.

Herrmann, J.T., Casana, J., Qandil, H.S., 2012. A sequence of inland desert settlement in the Oman peninsula: 2008–2009 excavations at Saruq al-Hadid, Dubai, U.A.E. Arabian Archaeol. Epigr. 23 (1), 50–69.

Hester, J., Hamilton, J.R., Rahbini, A., Eskoubi, K.M., Khan, M., 1984. Preliminary report on the third phase of ancient mining survey southwestern province – 1043 AH 1983. Atlal 8, 115–141.

Højlund, F., Andersen, H.H., Callot, O., 1994. Qala'at Al-Bahrain. Aarhus University Press, Aarhus.

Højlund, F., Andersen, H.H., 1997. Qala'at Al-Bahrain 2: the Central Monumental Buildings. Aarhus University Press, Aarhus.

Howari, F., Baghdady, A., Goodell, P., 2007. Mineralogical and gemorphological characterization of sand dunes in the eastern part of United Arab Emirates using orbital remote sensing integrated with field investigations. Geomorphology 83, 67–81.

Ingo, G., Mazzoni, S., Bultrini, G., Fontana, S., Padeletti, G., Chiozzini, G., Scoppio, L., 1994. Small-area XPS and XAES study of the iron ore smelting process. Surf. Interface Anal. 22 (1-12), 614–619.

Jasim, S., 2012. The necropolis of Jebel al-Buhais: prehistoric discoveries in the emirate of Sharjah, United Arab Emirates. Department of Culture and Information, Government of Sharjah, U.A.E.

Karacic, S., Händel, M., Hammer, E., Magee, P., 2018a. The architecture of the Iron Age II fortified settlement at Muweilah (Sharjah, United Arab Emirates). Arabian Archaeol. Epigr. 29, 27–54.

Karacic, S., Weeks, L., Cable, C., Méry, S., al-Ali, Y., Boraik, M., Zein, H., Glascock, M.D., MacDonald, B.L., 2018b. Integrating a complex late prehistoric settlement system: neutron activation analysis of pottery use and exchange at Saruq al-Hadid, United Arab Emirates. J. Archaeol. Sci. Rep 22, 21–31.

Killick, D, 2014. From Ores to Metals. In: Roberts, B, Thornton, C (Eds.), Archaeometallurgy in Global Perspective. Springer, New York, pp. 11–45.

Leroy, S, 2010. Circulation au Moyen Âge des matériaux ferreux issus des Pyrénées ariégeoises et de la Lombardie. Apport du couplage des analyses en éléments traces et multivariées. PhD Thesis. Université de Technologie de Belfort-Montbeliard.

Leroy, S., Cohen, S., Verna, C., Gratuze, B., Téreygeol, F., Fluzin, P., Bertrand, L.E., Dillmann, P., 2012. The medieval iron market in Ariège (France). Multidisciplinary analytical approach and multivariate analyses,. J. Archaeol. Sci. 39, 1080–1093.

Lippard, S., Shelton, A., Gass, I., 1986. The Ophiolite of Northern Oman. Geological Society of London Memoir 11. Blackwell Scientific Publications, Oxford.

Lombard, P., 1989. Âges du fer sans fer: le cas de la péninsule d'Oman au 1er millénaire avant JC. In: Fadh, J.-C.T. (Ed.), L'Arabie préislamique et son environnement historique et culturel : actes du Colloque de Strasbourg, 24-27 juin 1987. Brill, Leiden, pp. 25–37.
Lombard, P., Kervan, M., 1989. In: Bahrain National Museum Archaeological Collections, Vol. 1. A Selection of Pre-Islamic Antiquities from Excavations 1954-1975. Ministry of Information, Bahrain.
Magee, P., 1998. New evidence of the initial appearance of iron in southeastern Arabia. Arabian Archaeol. Epigr. 9, 112–117.
Magee, P., 1999. Writing in the Iron Age: the earliest south Arabian inscription from southeastern Arabia. Arabian Archaeol. Epigr. 10, 43–50.
Magee, P., Thompson, E., Mackay, A., Kottaras, P., Weeks, L., 2002. Further evidence of desert settlement complexity: report on the 2001 excavations at the Iron Age site of Muweilah, Emirate of Sharjah, United Arab Emirates. Arabian Archaeol. Epigr. 13, 133–156.
Magee, P., 2003. Columned halls, power and legitimisation in the southeast arabian iron age, archaeology of the United Arab Emirates. In: Proceedings of the First International Conference on the Archaeology of the U.A.E. Trident, London, pp. 181–191.
Magee, P., Lamberg-Karlovsky, C., Grave, P., 2004. Excavations at Tepe Yahya, Iran 1967-1975: the Iron Age Settlement. Harvard University, Harvard.
Magee, P., 2005. The production, distribution and function of Iron Age bridge-spouted vessels in Iran and Arabia: results from recent excavations and geochemical analysis. Iran 43, 93–115.
Magee, P., 2010. Iran and the Gulf in the first half of the first millennium BC. In: Avanzini, A. (Ed.), Eastern Arabia in the first millennium B.C. L'Erma di Brettschneider, pp. 45–56. Rome.
Magee, P., 2013. Iron Age southeastern Iran. In: Potts, D.T. (Ed.), The Oxford Handbook of Ancient Iran. Oxford University Press, Oxford.
Magee, P., 2014. The Archaeology of Prehistoric Arabia: Adaptation and Social Formation from the Neolithic to the Iron Age. Cambridge University Press, Cambridge.
Malkani, M.S., Mahmood, Z., 2016. Mineral resources of Pakistan: a review. Geological Survey of Pakistan.
Maresca, G., 2018. Between 'early' and 'late' Iron Age in South-eastern Iran: notes on the possibility to evaluate the 'Achaemenid impact' on the area. Vicino Oriente XXII 197–211.
Maxwell-Hyslop, K., Mallowan, M., 1974. Assyrian sources of iron. Iraq 36, 139–154.
McDonnell, J., 1991. A model for the formation of smithing slags. Materialy Archeologiczne 26, 23–26.
McDonough, W.F., Sun, S.-S., 1995. The composition of the earth, chem. Geol. 120, 223–253.
Meshram, R., Randive, K., 2011. Geochemical study of laterites of the Jamnagar district, Gujarat, India: implications on parent rock, mineralogy and tectonics. J. Asian Earth Sci. 42, 1271–1287.
Miroschedji, P.D., 1981. Fouilles du chantier Ville Royale II à Suse (1975-1977). I. Les niveaux élamites. Cahiers de la Délégation Archéologique Française en Iran (DAFI) 15, 9–136.
Mollaei, H., Yaghubpur, A., Attar, R.S., 2009. Geology and geochemistry of skarn deposits in the northern part of Ahar batholith, East Azarbaijan, NW Iran. Ir. J. Earth Sci. 1, 15–34.
Momenzadeh, M., 2004. Metallic mineral resources of Iran, mined in ancient times: a brief review. In: Stöllner, T., Slotta, R., Vatandoust, A. (Eds.), Persiens Antike Pracht. Bergbau - Handwerk - Archäologie. Katalog der Ausstellung des Deutschen Bergbau-Museums Bochums von 28. Deutsches Bergbau-Museum, Bochum, pp. 8–21.
Moorey, P.R.S., 1994. Ancient Mesopotamian Materials and Industries: the Archaeological Evidence. Clarendon Press, Oxford.
Moufti, A., 2010. Field, mineralogical and geochemical characteristics of As-Sarat laterite profiles. SW Saudi Arabia. J. King Abdulaziz Univ. Earth Sci. 21 (2), 47–75.
Muscarella, O., 1988. Bronze and Iron: Ancient Near Eastern Artifacts in the Metropolitan Museum of Art. Metropolitan Museum of Art, New York.
Nabatian, G., Rastad, E., Neubauer, F., Honarmand, M., Ghaderi, M., 2015. Iron and Fe–Mn mineralisation in Iran: implications for Tethyan metallogeny, Aust. J. Earth Sci. 62, 211–241.
Nashef, K., 2010. An industrial complex of the Iron Age II period. Saruq al Hadid. In: Avanzini, A. (Ed.), Eastern Arabia in the first millennium B.C. L'Erma di Brettschneider, Rome, pp. 213–226.
Overlaet, B., 2003. The Early Iron Age in Pusht-I Kuh, Luristan, Luristan Excavation Documents IV. Peeters, Leuven.
Overlaet, B., 2004. Metallarbeiten aus dem Luristan der Eisenzeit. In: Stöllner, T., Slotta, R., Vatandoust, A. (Eds.), Persiens Antike Pracht. Bergbau - Handwerk - Archäologie. Katalog der Ausstellung des Deutschen Bergbau-Museums Bochums von 28. Deutsches Bergbau-Museum, Bochum, pp. 328–338.
Overstreet, W.C., Domenico, J., Grolier, M., Tibbitts Jr., G., Ibrahim, M., 1976. Trace Elements in Some Rocks and Slag from the Yemen Arab Republic and Their Bearing on the Iron Ore Near Sa'dah. US Geological Survey.
Petrie, C.A., Asgari-Chaverdi, A., Seyedin, M., 2009. Excavations at Tol-E Spid. In: Potts, D., Roustaei, K., Petrie, C., Weeks, L. (Eds.), The Mamasani Archaeological Project Stage 1: the ICHTO/Sydney University Archaeological Research Project in the Mamasani Region. Fars Province, Iran. Archaeopress, Oxford, pp. 89–134.
Pigott, V., 2004. Hasanlu and the emergence of iron in early 1st millennium BC western Iran. In: Stollner, T., Vatandoost, T. (Eds.), Persiens Antike Pracht. Bergbau - Handwerk - Archäologie. Katalog der Ausstellung des Deutschen Bergbau-Museums Bochums von 28. Deutsches Bergbau-Museum, Bochum, pp. 350–357.
Pleiner, R., Bjorkman, J.K., 1974. The Assyrian Iron Age: the history of iron in the Assyrian civilization. Proc. Am. Phil. Soc. 118 (3), 283–313.
Ploquin, A., Orzechowski, S., Briand, B., 1999. Paléométallurgie à Mleiha: une première approche. In: Mouton, M. (Ed.), Mleiha I. Environnement, Stratégies de subsistance et artisanats. Maison de l'Orient méditerranéen, Lyon, pp. 171–190.
Potts, D., 1985. From Qadê to Mazûn: four notes on Oman, c. 700 BC to 700 AD. J. Oman Stud. 8 (1), 81–95.
Potts, D.T., 2009b. The archaeology and early history of the Persian Gulf. In: Potter, L. (Ed.), The Persian Gulf in History. Springer, Palgrave Macmillan, London, pp. 27–56.
Potts, D.T., 2012. In the Land of the Emirates: the Archaeology and History of U.A.E. Trident Press, Abu Dhabi.
Potts, D.T., 2004. The Archaeology of Elam: Formation and Transformation of an Ancient Iranian State. Cambridge University Press, Cambridge.
Potts, D.T., 2009. Urartian and Assyrian echoes at Saruq al-Hadid (emirate of Dubai). Liwa 2, 3–9.
Prange, M., Hauptmann, A., 2001. The Chemical Composition of bronze objects from 'Ibrī/Selme. In: Yule, P., Weisgerber, G. (Eds.), The Metal Hoard from 'Ibrī/Selme. Franz Steiner Verlag, Sultanate of Oman, pp. 75–87.
Rabinovich, A., Yahalom-Mack, N., Garfinkel, Y., Ganor, S., Hasel, M.G., 2019. The metal assemblage from early Iron Age IIA Khirbet Qeiyafa and its implications for the inception of iron production and use. Bull. Amer. Sch. Orient. Res. 382 (1), 89–110.
Rajabzadeh, M.A., Parvin, S., Nasab, Z.M., Dehkordi, R.S., 2012. Investigation of the origin of Heneshk Hematitic iron deposit, Fars province using petrological, mineralogical and geochemical data. Petrology 11, 1–20 (in Farsi).
Rice, M., 1988. Al Hajjar revisited: the grave complex at Al Hajjar, Bahrain (report revised, with photographs, 1988). Proceed. Seminar Arabian Stud. 18, 79–94.
Robins, N, Benham, A.J., Mitchell, C., 2006. The geology and geophysics of the United Arab Emirates. Volume 3, Economic geology and hydrogeology. Ministry of Energy, Abu Dhabi, United Arab Emirates.
Rostoker, W., Bronson, B., 1990. Pre-industrial Iron: Its Technology and Ethnology, 1st. Archeomaterials, Philadelphia.
Sasso, M., 2018. Metal objects. In: Avanzini, A., Esposti, D.E. (Eds.), Husn Salut and the Iron Age of South East Arabia. L'Erma di Bretschneider, Rome, pp. 301–330.
Serneels, V., 1993. Archéométrie des scories de fer: recherches sur la sidérurgie ancienne en Suisse occidentale. Cahiers d'archéologie romande, Lausanne.
Serneels, V, Perret, S, 2003. Quantification of smithing activities based on the investigation of slag and other material remains. In: Archaeometallurgy in Europe-Proceedings of the International Conference, 24-26 September 2003. Associazione Italiana di Metallurgia Milaan, Milan, Italy, pp. 469–478.
Skoček, V., Al-Qaraghuli, N., Saadallah, A.A., 1971. Composition and sedimentary structures of iron ores from the Wadi Husainiya area, Iraq. Econ. Geol. 66, 995–1004.
Smith, C.S., 1971. The techniques of the Luristan smith. Science and archaeology 32–52.
Sperveslage, G., 2016. Intercultural contacts between Egypt and the Arabian Peninsula at the turn of the 2nd to the 1st millennium BCE. In: Moreno García, J.C. (Ed.), Dynamics of Production in the Ancient Near East 1300–500 BC. Oxbow, Oxford, pp. 303–330.
Srinivasan, S., Ranganathan, S., 2004. India's Legendary Wootz Steel: an Advanced Material of the Ancient World, National Institute of Advanced Studies and Indian Institute of Science, Bangalore.
Stepanov, I., Borodianskiy, K., Eliyahu-Behar, A., 2020. Assessing the quality of iron ores for bloomery smelting: laboratory experiments. Minerals 10, 33, 1–25. https://doi.org/10.3390/min10010033.
Stepanov, I., Weeks, L., Franke, K., Cable, C., Overlaet, B., Magee, P., Händel, M., Al Aali, Y., Radwan, M., Zein, H., 2017. Methodologies for the investigation of corroded iron objects: examples from prehistoric sites in South-eastern Arabia and western Iran. Star: Science & Technology of Archaeological Research 3 (2), 270–284. https://doi.org/10.1080/20548923.2018.1424304.
Stepanov, I., Weeks, L., Franke, K., Salvemini, F., Cable, C., Al Ali, Y., Radwan, M., Zein, H., Grave, P., 2019a. Scrapping ritual: Iron Age metal recycling at the site of Saruq al-Hadid (U.A.E.). J. Archaeol. Sci. 101, 72–88.
Stepanov, I., Weeks, L., Salvemini, F., Al Ali, Y., Radwan, M., Zein, H., Grave, P., 2019. Early Iron Age ferrous artefacts from southeastern Arabia: investigating fabrication techniques using neutron tomography, optical microscopy and SEM-EDS. Anthropol. Archaeol. Sci. 11 (6), 2971–2988.
Taha, M.Y., 2009. The discovery of the Iron Age in the United Arab Emirates. Ministry of Culture. Youth and Community Development, Abu Dhabi.
Tewari, R., 2003. The origins of iron working in India: new evidence from the Central Ganga Plain and the eastern Vindhyas. Antiquity 77, 536–544.
Tewari, R., 2010. Updates on the antiquity of iron in south Asia. Man and Environment 35 (2), 81–97.
Van De Mieroop, M., 2007. A History of the Ancient Near East Ca. 3000–323 BC. MA. Blackwell, Malden.
Van de Velde, Th., Magee, P., Lynen, F., 2017. The bitumen imports at Tell Abraq: tracing the second millennium BC bitumen industry in south-east Arabia. Proceed. Seminar Arabian Stud. 47, 227–238.
Velde, C., 2003. Wadi Suq and Late Bronze Age in the Oman peninsula. In: Potts, D.T., Al-Naboodah, H., Hellyer, P. (Eds.), Archaeology of the United Arab Emirates. Trident, London, pp. 101–114.
Veldhuijzen, H., 2005. Early iron production in the Levant, PhD dissertation.
Veldhuijzen, H.A., Rehren, T., 2007. Slags and the city: early iron production at Tell Hammeh, Jordan, and Tel Beth-Shemesh. Israel. In: La Niece, S., Hook, D., Craddock, P. (Eds.), Metals and Mines: Studies in Archaeometallurgy. Archetype Publications, London, pp. 189–201.
Waldbaum, J.C., 1999. The coming of iron in the eastern Mediterranean: thirty years of archaeological and technological research. In: Pigott, V.C. (Ed.), Archaeometallurgy of the Asian Old World. Museum University of Pennsylvania, Philadelphia, pp. 27–58.

Weeks, L., 2003. Early metallurgy of the Persian Gulf: technology, trade, and the Bronze Age World. Brill, Boston.

Weeks, L.R., Alizadeh, K., Niakan, L., Alamdari, K., Khosrowzadeh, A., Zeidi, M., 2009. Excavations at Tol-e Nurabad. In: Potts, D.T., Roustaei, K., Petrie, C.A., Weeks, L.R. (Eds.), The Mamasani Archaeological Project Stage 1. The ICHTO/Sydney University Archaeological Research Project in the Mamasani Region, Fars Province, Iran. Archaeopress, Oxford, pp. 31–88.

Weeks, L., Cable, C., Franke, K., Newton, C., Karacic, S., Roberts, J., Stepanov, I., David-Cuny, H., Price, D., Bukhash, R.M., Radwan, M.B., Zein, H., 2017. Recent archaeological research at Saruq al-Hadid, Dubai, U.A.E. Arabian Archaeol. Epigr. 28, 31–60.

Weeks, L., Cable, C., Franke, K., Newton, C., Karacic, S., Roberts, J., Stepanov, I., David-Cuny, H., Price, D., Yousif Al Aali, Y., Radwan, M.B., Zein, H., 2019a. Saruq al-Hadid: a persistent temporary place in late prehistoric Arabia. World Archaeol. 50, 1–26.

Weeks, L., Cable, C., Karacic, S., Franke, K., Price, D., Newton, C., Roberts, J., Al Ali, Y., Boraik, M., Zein, H., 2019b. Dating Persistent Short-Term Human Activity in a Complex Depositional Environment: Late Prehistoric Occupation at Saruq Al-Hadid. Radiocarbon, Dubai.

Weisgerber, G., 2008. Metallurgy in Arabia. In: Selin, H. (Ed.), Encyclopaedia of the History of Science, Technology, and Medicine in Non-western Cultures, 2nd. Springer: Kluwer Academic Publishers, Netherlands, pp. 1613–1622.

Wilson, R.A., 1997. Geochemistry of Metalliferous Sediments from the Northern Oman Ophiolite. PhD Thesis. Durham University.

Wimpenny, J., Gannoun, A., Burton, K., Widdowson, M., James, R., Gíslason, S., 2007. Rhenium and osmium isotope and elemental behaviour accompanying laterite formation in the Deccan region of India. Earth Planet. Sci. Lett. 261 (1-2), 239–258.

Yule, P., Weisgerber, G., 2015. Al-wāsiṭ tomb W1 and other sites, materials for a definition of the second half of the 2nd millennium BCE. In: Yule, P. (Ed.), Archaeological Research in the Sultanate of Oman. Vml Verlag Marie Leidorf, Rahden, pp. 9–108.

Yule, P., 2018. The finds. In: Yule, P., Gernez, G. (Eds.), Early Iron Age Metal-Working Workshop in the Empty Quarter, Al-Ẓāhira Province, Sultanate of Oman. Verlag Dr. Rudolf Habelt GmbH, Bonn, pp. 33–147.

Zamanian, H., Radmard, K., 2016. Geochemistry of rare earth elements in the Baba Ali magnetite skarn deposit, western Iran–a key to determine conditions of mineralisation. Geologos 22 (1), 33–47.

Zamanian, H., Yeganeh, B.Y., Alavi, S., 2007. Mineralogical and geochemical skarn zoning across the Baba Ali deposit and its economic geology applications, western Iran. Geosciences 16 (62), 194–202.

Zarasvandi, A., Lentz, D., Rezaei, M., Pourkaseb, H., 2013. Genesis of the Nasirabad manganese occurrence, Fars province, Iran: geochemical evidences. Chem. Erde-Geochem. 73 (4), 495–508.

Zarins, J.N., Whalen, M., Ibrahim, A. Morad, Khan, M., 1980. Comprehensive archaeological survey program – preliminary report on the central and southwestern provinces survey. Atlal 4, 9–36.